Microstructure Evaluation of Copper Prepared through Fused Deposition Modelling of Metal

By

Muzamil Ahmad Shabbir

00000203995

Supervisor

Dr. Emad Uddin

SCHOOL OF MECHANICAL & MANUFACTURING ENGINEERING

NATIONAL UNIVERSITY OF SCIENCES AND TECHNOLOGY

ISLAMABAD

2020

Microstructure Evaluation of Copper Prepared through Fused Deposition Modelling of Metal

By

Muzamil Ahmad Shabbir

00000203995

A thesis submitted in partial fulfillment of the requirements for the degree of

MS Mechanical Engineering

Supervisor

Dr. Emad Uddin

Thesis Supervisor's Signature: _____

SCHOOL OF MECHANICAL & MANUFACTURING ENGINEERING

NATIONAL UNIVERSITY OF SCIENCES AND TECHNOLOGY, ISLAMABAD

2020

THESIS ACCEPTANCE CERTIFICATE

Certified that final copy of MS/MPhil thesis written by **Mr. Muzamil Ahmad Shabbir**, (Reg. No. **00000203995**), of **SMME** (School/College/Institute) has been vetted by undersigned, found complete in all respects as per NUST Statutes/Regulations, is free of plagiarism, errors and mistakes and is accepted as partial fulfillment for award of MS/MPhil Degree. It is further certified that necessary amendments as pointed out by GEC members of the scholar have also been incorporated in the said thesis.

Signature: _____

Name of Supervisor: **Dr. Emad Uddin**

Date: _____

Signature (HOD): _____

Date: _____

Signature (Principal): _____

Date: _____

National University of Sciences & Technology
MASTER THESIS WORK

We hereby recommend that the dissertation prepared under our supervision by: (Student Name & Regn No.) Muzamil Ahmad Shabbir & 00000203995 Titled: Microstructural Evaluation of Copper Prepared Through Fused Deposition Modelling of Metal be accepted in partial fulfillment of the requirements for the award of MS Mechanical Engineering degree.

1.   Name: Dr. Aamir Mubashar   Signature: _____

2.   Name: Dr. Zaib Ali   Signature: _____

3.   Name: Dr. Samiur Rahman Shah   Signature: _____

Supervisor's name: Dr. Emad Uddin   Signature: _____
Date: _____

_____   _____

Head of Department   Date

COUNTERSINGED

Date: _____   _____
Dean/Principal

Declaration

I certify that this research work titled *"Microstructure Evaluation of Copper Prepared through Fused Deposition Modelling of Metal"* is my individual work. The work has not been presented elsewhere for evaluation. The material that has been used from other sources it has been adequately acknowledged / referred.

Signature of Student

Muzamil Ahmad Shabbir

00000203995

Plagiarism Certificate (Turnitin Report)

This thesis has been checked for Plagiarism. Turnitin report endorsed by Supervisor is attached.

Muzamil Ahmad Shabbir

00000203995

Signature of Supervisor

Dr. Emad Uddin

Copyright Statement

Acknowledgements

The utmost beneficial and the Greatest ALLAH Almighty has always showered his endless blessings upon me. All gratitude and attributes to Him, who helped me to complete my thesis.

I am obliged to the tremendous support and guidance provided at every step throughout this interval by my supervisor Dr. Emad Uddin. Without his cooperation and assistance, I would have been totally incapable to carry out this research work so easily.

I am abundantly thankful to the GEC members which comprises of Dr. Aamir Mubashar, Dr. Zaib Ali & Dr. Sami ur Rehman Shah for their constant help.

The insightful suggestions, motivation, unceasing support and prayers of my siblings & friends who made it possible for me to fulfill this work with devotion and enthusiasm.

Last but not the least, I am profusely thankful to my beloved parents who raised me when I was not capable of walking and continued to support me throughout in every department of my life.

Abstract

Metal-based additive manufacturing, or three-dimensional (3D) metal printing, is a relatively new technique having potential to enable manufacturers to print small metallic parts directly rather than adopting the traditional casting method. The application of additive manufacturing is present across various industries, aerospace industry being on of the largest research group. This technique enables one to build complex geometries by increasing the degrees of freedom of design and further removes the need of after-treatment such as cutting, sanding etc. after the manufacturing. Various techniques are currently being used which include selective laser melting, electron beam melting to print metallic parts from the powdered metal. However, these techniques provide a costly solution and that is not feasible for small industries. In this thesis a new technique will be discussed. A research study was carried out to develop metallic components by combining Fused Deposition Modelling with Sintering technique. The objective of study was to evaluate the use of this approach as an alternative to casting. Small coupons of copper filament were printed and sintered for different deposition strategy and sintering time durations according to design of experiment (DOE) technique. After sintering, microstructure of coupons was studied by metallography technique and comparison was drawn between coupons. Moreover, micro hardness test was also performed to estimate the ultimate tensile strength of 3D printed copper. The grain structure and micro hardness was found to be in comparison with the casted copper however, there was non-uniformity in the grain structure as some areas still had large voids present. In light of the result obtained, optimized parameter for producing copper parts using FDMet process were recommended. The process has potential of manufacturing fully functional metal parts and can be implemented as an alternative to casting process in all engineering fields however shrinkage needs to be catered in the initial CAD model.

Table of Contents

List of Figures

List of Tables

Chapter 1:   Introduction

1.1 Background

The use of 3D printing technology dates to early 80's when prototypes of different engineering designs were manufactured using said technique. It was an important advancement in prototype manufacturing which not only increased the efficiency of design process by visual depiction of initial design but also reduced the total time needed for finalization of product design. The evolution of 3D printing technology yielded new benefits in 1900's including but not limited to use in reverse engineering process and additive manufacturing. With latest advancement, 3D printing is now possible for manufacturing using various polymers / thermoplastic materials such as Polylactide (PLA), Acrylonitrile Butadiene Styrene (ABS) and metals also, that are proving helpful in modern engineering (Additive, 2020). The revolution of manufacturing process relies significantly on additive manufacturing (AM), it aims to provide manufacturers cost effective solution without compromising on strength and quality of the manufactured product. Automotive industries have started to adopt this technology with Bugatti being the pioneer in using 3D printed / Additive manufacturing technique to manufacture its titanium brake caliper (Frazier, 2014). Similarly, efforts are being made to use this technology in the aerospace and defense industry, although number of parts manufactured through AM are already flying in Boeing Aircrafts but the technology still needs to be developed before depending completely on additive manufacturing. AM has help to reduce the cost of new tools and saves time of work completion. It also eradicates the limitations that prevent the optimal design, innovations, and makes the production of complex part easy to design (Gokuldoss, Kolla, & Eckert, 2017). Various techniques commonly used in additive manufacturing and their respective material compatibility is given in table 1.

Materials	Techniques			
	Binder Jetting (BJ)	Laser Sintering / Melting (LS / LM)	Electron Beam Melting (EBM)	Fused Deposition Modelling (FDM)
Ceramic	✓	✓	✗	✗
Metal	✓	✓	✓	✓
Sand	✓	✗	✗	✗
Plastic	✓	✓	✗	✓

Table 1. 1: Material Compatibility of Various Additive Manufacturing Techniques

1.2 Aim & Objective

The main aim of the research work which is being discussed here is to manufacture copper coupons through Fused Deposition Modelling technique and examine the microstructure through which various parameters like accumulation area, void area and density of the coupons can be calculated.

Several objectives are laid down to fulfill the above stated aim.

➢ To develop metal coupons using the Fused Deposition Modelling (FDMet) technique.

➢ To investigate the effect of build parameters i.e sintering time and deposition strategy on end result by material characterization (Microstructure, Composition etc.) of coupons obtained

➢ To carry out image analysis to obtain accumulation area and void / throat size distribution

➢ To evaluate the Hardness of obtained coupons and carry out comparison with casted copper.

➢ Step by step documentation of research work so that future students can do further research in the field of Fused Deposition Modelling of metals efficiently.

The material used for the Fused Deposition Modelling was Copper Filament with 90% copper grains and 10% PLA as binder.

1.2 Research Methodology

The research work has been divided into various stages which start from the development of green part through fused deposition modelling. Subsequently, the green parts were sintered in an atmospheric furnace to obtain pure copper parts for material characterization Experimental work was carried out at SMME, NUST to study the microstructure and hardness of the sintered samples and calculate other desired parameters in parallel with the numerical work. The image analysis was carried out using a MATLAB algorithm, the distribution of copper accumulation and throat was determined. From these measured and predicted results, conclusions were drawn in relation of different layer heights and sintering time duration against maximum copper accumulation area.

Framework for the research work is given below in the Figure 1.1.

Literature Review
- DSLS & DSLM
- 3D Printing
- FDMet

Development of DOE
- Levels (No. of Exp)
- Variables (Sintering Time)
- Performance Parameter

3D Printing
- Deposition Strategy
- Printing Parameters
- Nozzle Size

Sintering
- Sintering Technique
- Candling & Debinding
- Sintering Cycle

Characterization
- Metallography
- Hardness & Porosity
- Composition

Results & Discussion
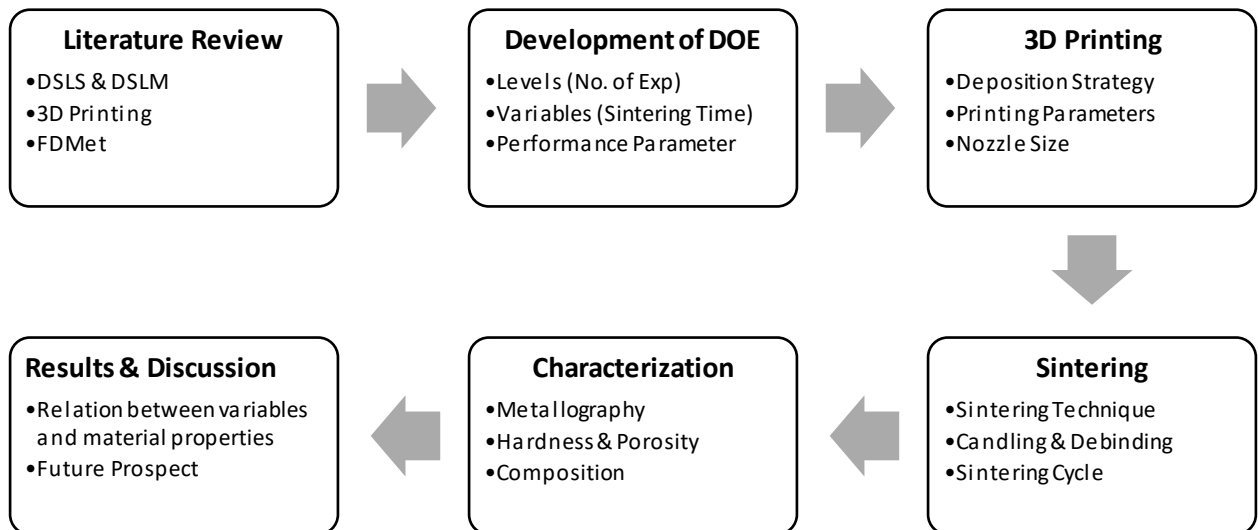- Relation between variables and material properties
- Future Prospect

Figure 1. 1 Research Methodology

1.3 Thesis Layout

A brief description of the chapters of the thesis has been given as follows:

Chapter 1: Introduction

Introduction of the research topic along with the significance and major aims and objectives of the research work are discussed in this chapter. It contains the research methodology as how the research work has been divided into various stages.

Chapter 2: Literature Review

Foundation of the research carried out in this thesis is laid down in this chapter. Firstly, different techniques for the additive manufacturing are discussed along with their benefits and drawbacks. In second part, basics of fused deposition modelling technique are explained. Finally, research work on metal parts manufacturing through FDMet process and mechanism by different researchers has been discussed.

Chapter 3: Experiment Methodology

Based on the literature review, experimental methodology for the research is explained in this chapter. Parameters for producing optimized green parts through simple 3D printer is given in this chapter. Development of DOE table for this study, and details on variables opted for the study are also explained in this chapter.

Chapter 4: Sintering Process

This chapter explains the equipment and sintering process, which is carried out at Heat Treatment Lab, SMME, NUST. It includes the details of pre sintering process and sintering cycle used for current study.

Chapter 5: Results and Discussions

This chapter gives an overview of the results through different experiments and obtained values for shrinkage, hardness & density etc. Comparison between copper accumulation area at different layer heights and different sintering duration is explained through graphs and charts.

Chapter 6: Conclusion and Future Works

Conclusions drawn from the research carried out are presented in this chapter. Also it contains the area of further development and proposal for future work.

Chapter 2: Literature Review

3D printing of metals can be performed using powder bed system, powder feed system and wire feed system. Powder bed system is the most commonly used process, which is further categorized into Electron Beam Melting, Direct Metal Laser Sintering (DMLS), and Direct Metal Laser Melting (DMLM). These aforementioned techniques are specifically for metals. The two latter are inferred from Selective Laser Sintering (SLS) and Selective Laser Melting (SLM) also referred as Laser Powder Bed Fusion (LPBF). DMLS and DMLM are quite similar process except for fact the degree to which the metal is heated. In Direct Metal Laser sintering process, the powder is heated to a certain temperature (sintering temperature) that is less than melting point of that metal using a laser beam. This causes particles to fuse and link with one another. Powder is sintered into ultra-fine layers initially on a substrate plate and subsequently over one another to obtain the required part. On the other hand, laser in DMLM process causes powder to completely melt and create micro liquid channels that solidify as they cool. Similarly, layers are then arranged to dictate the CAD model (Frazier, 2014) The process is carried out in a closed chamber, to avoid formation of metal oxides this chamber is filled with some inert gas such as Argon which varies depending on the material being used. Another practice adopted to inhibit reactivity is external pressure conditions. A base plate is also present inside the chamber, this plate is used to avoid rapid cooling of the material having high melting points. This averts any hot cracking that may occur along grain boundaries during solidification due to thermal contraction (Prashanth K.G., 2015). The precision of parts manufactured by both DMLS and DMLM are in accordance with the quality tolerances even for complex parts. However, a number of factors need to be controlled for manufacturing of a part with optimized / required characteristics (Schwab, Prashanth, Löber, Kühn, & Eckert, 2015) (Laakso, et al., 2016)[48,50]. One main factor in this case is laser specification and height of each fused layer. For DMLS no support structure is required, and residual stresses are not an issue. However, to cater shrinkage due to sintering, temperature of chamber can be heated to a point just below the sintering temperature for certain low metal alloys. The only challenge associated with DMLS is porosity of manufactured parts that needs to be resolved by using a sealant or adhesive. On contrary, precise parts manufactured by DMLM can show accurate microstructure arrangement with surface finish and mechanical properties resembling to casted counterpart. With proper support structures to restrict any distortion that may occur in part due to high

temperature induced stresses, it is possible to achieve approximately 100% density using the DMLM process. With latest DMLM technology, the bed permits to print part with a layer height of only 20 microns enabling manufacturer to create parts with short lead times and more degree of freedom as compared to traditional methods (Additive, 2020). Moreover, these DMLM parts require no / very little post processing procedures after manufacturing. DMLS and DMLM enables printing of variety of metals that include Aluminum (Kimura, Nakamoto, Mizuno, & Araki, 2017), Titanium (Thijs, Verharghe, Craeghs, Humbeeck, & Kruth, 2010), Iron (Zhu, Chen, & Yang, 2016), Nickle (Lu, et al., 2015) and several other alloys. The basic techniques SLM & SLS however allow printing of both metal and amorphous materials (Jung, et al., 2015)[24]. Copper prepared by DMLM technique has a number. According to a study performed by Fraunhofer Institute for Laser Technology (Germany), quality printing of copper requires a laser that has a power rating of 300 W minimum (Meiners, 2011).
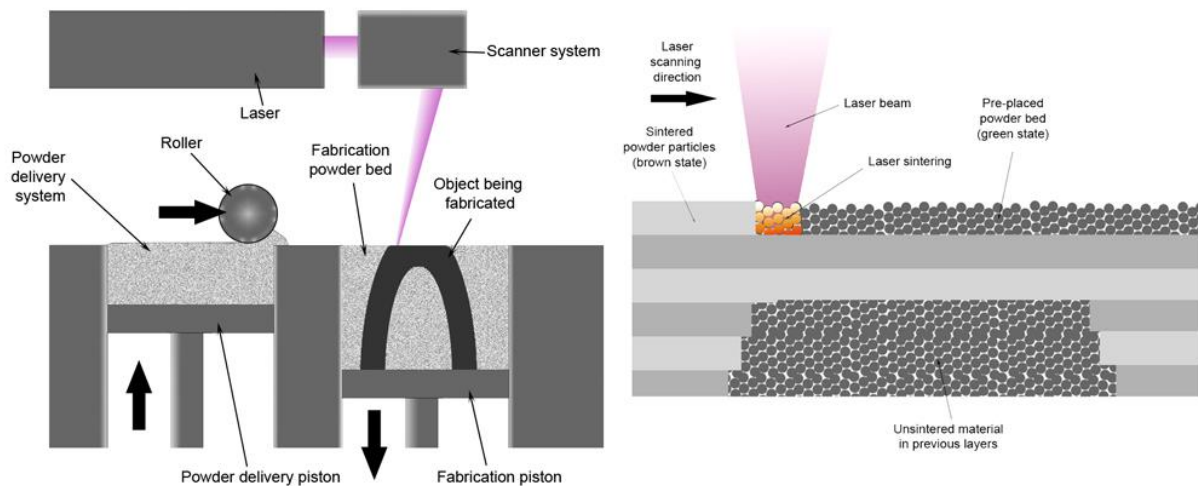

Figure 2. 1: Selective Laser Sintering Technique

Similar layer by layer fusion technique is also observed in Electron Beam Melting however, an electron beam is focused on metal powder instead of laser as in case of DMLS and DMLM. The base plate is also heated at a relatively higher temperature than in DMLM to prevent rapid cooling. In most times part is left overnight to cool at a moderate rate. This is done for catering the problem of hot cracking that occurs in DMLM, EBM technology offers better structure of brittle materials that have poor thermal expansion and contraction coefficients. The temperature of base plate is controlled in such a manner that there is no

drastic reduction in the temperature of build part that may cause solidification cracks. The temperature of base plate in DMLM has a range around $200 - 500$ C^o that too in some machines whereas, this temperature is greater than 600 C^0 for EBM printing (Gokuldoss, Kolla, & Eckert, 2017). Another difference lies in the environment of the enclosed chamber, the earlier mentioned technique had an inert environment whereas for EBM printing is done in a vacuum chamber. The purpose of vacuum is same as of inert gas that is avoiding any oxidation of metal. However, Elimination of porosity caused by adsorption of gases is also an added advantage of this vacuum chamber in case of EBM. Furthermore, the amount of stresses produced via EBM techniques are also comparatively lesser to that of laser melting. Although, EBM may seem a better option, yet it has some drawbacks. Just like DMLM or DMLS, EBM technique also have a number of variables such as beam focus & intensity, beam diameter etc. that need to be controlled for optimized results. The optimization of these parameters is difficult in case of EBM because of high temperature. Moreover, the range of materials that can be printed using the EBM technique is also limited and are generally titanium-based alloys. This technique is rather expensive than laser melting but is relatively faster. Another drawback of EBM is the requirement of post processing, parts manufacture by EBM have a surface finish of $20.3 - 25.4$ microns compared to $4 - 10$ microns obtained through laser melting (Electron Beam Melting, 2020).
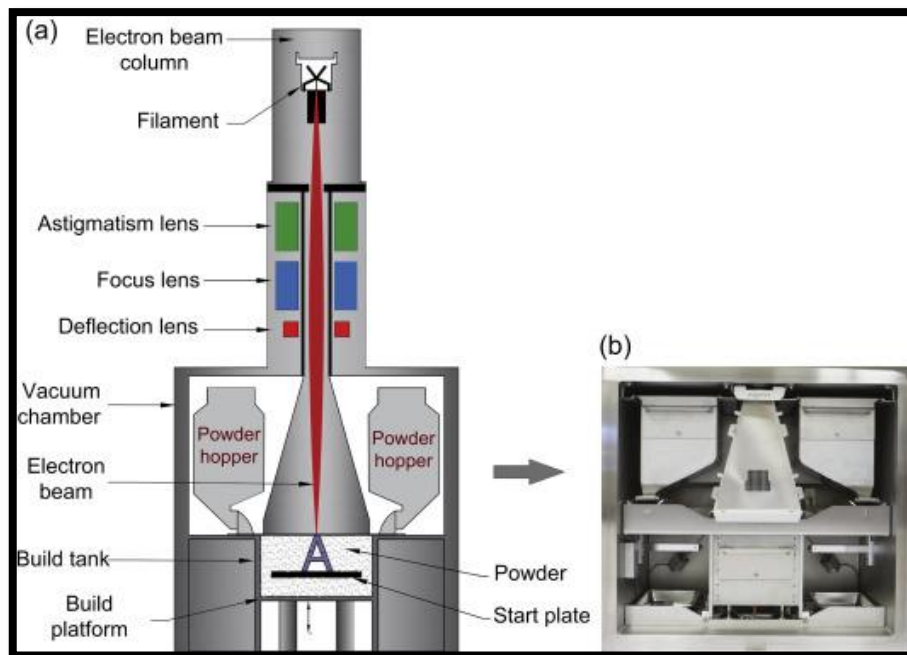

Figure 2. 2: Electron Beam Melting Technique

The technique focused in this research is a combination of two processes i.e Fused Deposition Modelling (FDM) and Sintering process and is referred as FDMet. Coming towards FDM, the technique was designed for plastic filament and Acrylonitrile Butadiene Styrene (ABS) and Polylactide (PLA) are the most commonly used filaments. The process is comparatively simpler and easy to understand. A motor pushes the filament into the nozzle, the nozzle is heated to a specific temperature depending on the type of filament and its melting temperature. With the help of controlled mechanism, the nozzle moves and prints the melted filament in layers on the printer bed. The layers are stacked on one another until the required part is manufactured. For plastic parts the process ends here, however sintering is required for metallic filaments that are made using a powder metal and binder for holding the powder metal in desired shape as in Binder Jetting. (Binder Jetting is an additive process in which two materials (a) powder material (b) binder are used. The printer deposits a layer of powder and binder in an alternate manner which causes different layers to bond together (University, n.d.). The develop part doesn't have the strength that is obtained through other additive manufacturing processes and therefore can't be used as structural part). The sintering of printed parts obtained through FDM causes the powder metal to fuse as in case of Selective Laser Sintering and also disintegrate the binder from the green print to obtain a pure metal. This process enables one to print 3D metal parts without using any laser source or Electron Beam.

Initial work regarding feasibility and optimization of printing of metal using FDM was done by Center for Ceramic Research, Rutgers University, they worked on the possibility of using ceramics and metals printed through FDM technique for use in various application such as tooling, structural and other functional components. In their study, a precipitation hardened stainless steel powder of type 630 was mixed with a RU1 binder composition (30% wax, 35% polymer, 20% elastomer, and 15% tackifier by weight) in a ratio of 60% and 40% by volume. The mixture was later extruded into a 0.070" diameter straight filament using the capillary extrusion process. Simple parts were printed using the FDMTM system at 110°C, these parts were then processed for binder removal and subsequently sintered at 1350°C for 1 hour in a mild reducing atmosphere (H2+N2). The sintered parts showed > 90% theoretical density but were exposed to internal delamination and cracking due to binder removal process (Agarwala, Weeren, Bandyopadhyay, Whalen, & Safari, 1996). Later in 1999, another study was carried to develop complex real-world parts using the FDM metal printing

technique. He extruded relatively longer filaments of stainless steel 17 – 4 PH, one with a spherical powder (22 microns) and other of irregular shape (10 microns) both mixed with Electro Ceramic Group (ECG2) binder (McNulty, Cornejo, Mohammadi, Danforth, & Safari, 1998). He optimized the build parameters of FDM such as Main flow, offset specifically for metals and concluded that the FDMet built parts had better accuracy as compared to those obtained through RTV molding (Langrana, Rangarajan S, & al., 1999) (Guohua, Noshir A., Rajendra, & Danforth, 2002). Although the print had higher dimensional accuracy, but the parameters related to binder burn out and sintering still needed to be workout for full functionality of the parts. The use of parts printed using FDMet was also extended to other applications such as injection molding and tooling inserts. Composite parts in their green form without any post processing burnout and sintering process were subjected to rapid tooling and afterwards used. In a study by S. H. Masood, inserts made of metal polymer composite were used for injection molding of high-quality thermoplastic materials. These inserts were printed from filament made up of iron (40% by volume) and nylon (60% by volume) using FDM process (Masood & Song, 2004) . In a further study of the said iron nylon composite, it was concluded that with each 10% by volume increase in iron particles the heat capacity of the composite reduces however this comes with a significant decrease in tensile strength also (Nikzad, Masood, & Groth, 2007)[12].

Where different studies were being carried out to use FDMet parts as structural and fully functional substitute in different areas, a research was carried out to study the feasibility of using FDM technique in electronic circuitry. Different commercially available low melting temperature solder alloys such as Bi36Pb32Sn31Ag1, Bi58Sn42, Sn63Pb37, Sn50Pb50, Sn60Bi40, Sn96.5Ag3.5. Solder composition was the key parameter controlling the print quality. Clogging, coarsening and agglomeration were the different issues that occurring using FDM of the aforementioned alloys. Nevertheless, solder alloy of composition Sn-Bi with non-eutectic behavior proved to be finest compared with other alloys. The study showed promising results in the application of FDMet in designing of efficient electric circuits, controlled single layer print was obtained through FDM which had straight lines with sharp 90º turns and some areas with smooth curvatures as well (Mireles, et al., 2013). Another study for fabrication of sensors using copper PLA filament fused deposition modeling was also carried out. Microstructure of 3d printed layer having an average thickness of 76 microns was studied, however presence of PLA significantly reduced the

conductivity of layer. With post processing like burnout the conductivity can be increased and there is a possibility of using FDMet for electronic sensor fabrication (Arivarasi & Kumar, 2016).

Recently, an innovative conceptual design was proposed for Fused Deposition Modelling of metals and advance ceramics. Rather than the traditional wire feed for FDM, Metal or ceramic powder will be the input which will be mixed with a binder by a plasticizer. The plasticizer will load the heated (200 C^o) mixture to injection cylinder, a vertical piston will extrude the material in the injection cylinder through a nozzle with a minimum diameter of 0.2 mm. In this design, feeder, injector and nozzle assembly will be fixed, a robotic table on which layers are deposited will move in 5 DOF (Parallel Kinematic Mechanism). One benefit of this design includes minimum binder requirement hence a lower porosity and shrinkage percentage after post processing (Giberti, Strano, & Annoni, 2016)[16]. In 2016, Fraunhofer Institute for Manufacturing Technology and Advanced Materials IFAM worked on non-beam-based additive manufacturing approach for metallic parts. They followed a similar approach of fabricating a polymer metal filament for printing by FDM process and subsequently sintering it to obtain metallic part. The optimization of printing and sintering parameters can promise high density metallic parts using deposition technique (Riecker, Clouse, Studnitzky, Andersen, & Kieback, 2016) [17]. A similar result was concluded in another study by B. Liu, Y. Wang, Z. Lin, T. Zhang, 316L stainless steel was printed using FDM and later sintered in an inert atmosphere. Porosity and lesser but comparative static strength properties related to AISI 316L and SLM 316L parts were observed which could be improved by optimizing the process (Liu, Wang, Lin, & Zhang, 2020)[18].

Based on the literature review it was determined that this technique has potential to allow manufacturers to print working structural part without having to invest in an expensive process (DMLM or EBM) and moreover very little work is done to optimize the FDMet process. In previous studies the sintering was also carried out in an inert atmosphere, a new approach will be followed in this study by sintering in an open-end atmosphere furnace. This will further reduce the constraint associated with FDMet process.

Chapter 3:   Methodology

3.1 Filament Specification

Copper metal from filament Virtual Foundry LLC containing 90 % copper while 10 % PLA as a binder by volume. The density associated to the filament as indicate by the manufacturer is 4600 kg/m^3 whereas the melting range is defined as 205-235°C (401-455°F). The diameter of the copper filament in this study was 1.75mm. The 3D printer used for printing of specimen was which is easily available and relatively inexpensive. The copper filament and 3D printer is shown in Figure 3.1.
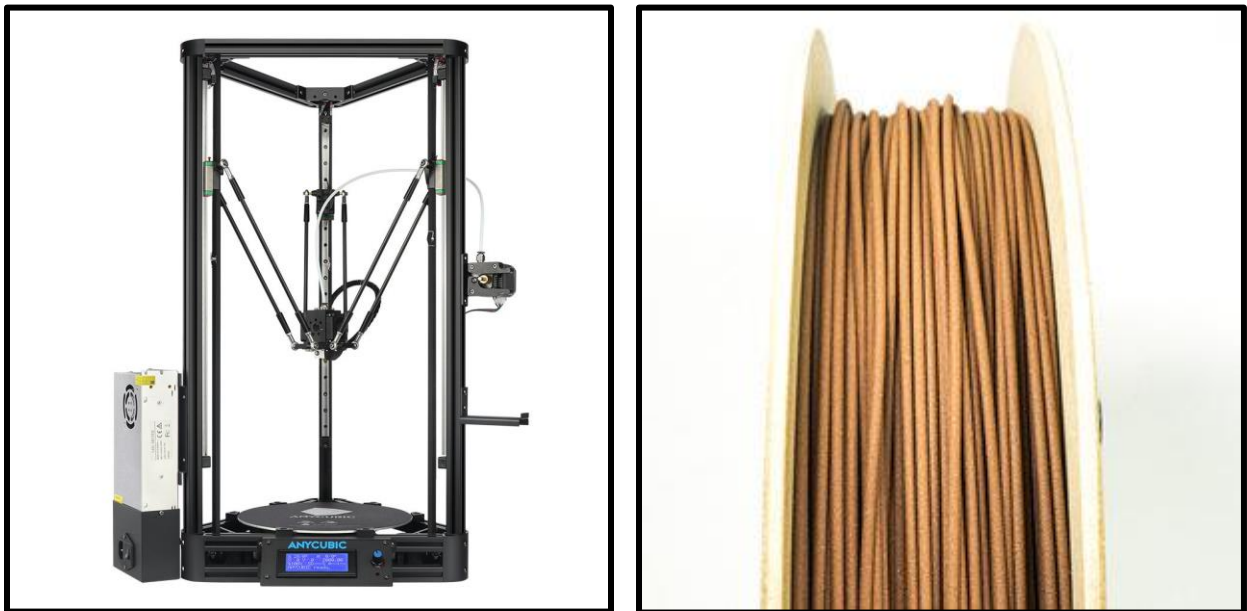
Figure 3. 1: 3D Printer & Copper Filament

3.2 Printing Parameters

The printing parameters carry key importance in Fused Deposition Modeling (FDM). As seen in literature, careful determination of these parameters is required for optimize printing of specimens. The cad model was imported in Cura 3D software for slicing and setting up the printing parameters. Initially the parameters indicated by Virtual Foundry were used, however the print obtained had intermittent layers as shown in Figure 3.2.

Figure 3. 2: Initial Print with Intermittent Layers

The printing speed was decreased from 30 mm/s to 25 mm/s and correspondingly flowrate was increased. A stainless-steel nozzle of size 0.4 mm was used for printing. Before every print the printer was calibrated to remove any zero error in the total height. The key parameters used in the printing process is given in table. These parameters can change depending upon the type of 3D printer used and may be altered as per the print quality. The infill percentage was set to 100% as the aim of the study was to use parts obtained through this strategy as fully functional replacements of the casted / machined parts. Reducing the infill would cause porosity, shrinkage and strength reduction of the final product.

Parameter	Value
Temperature	210 C^o
Printing Speed	25 mm/s

Infill Percentage	100%
Layer Height	0.1, 0.2 mm
Bed Temperature	40 C^o
Raft Use	Yes
Raft offset	15
Nozzle size	0.6 mm
Raster Angle	[0 , 90]
Flow Adjust	100%
Filament Diameter	1.75 mm
Raft layers	2
Raft Infill	30%
Fila Warmer	45 C^o

Table 3. 1: Finalized 3D Printer Input Parameters

3.3 Design of Experiment

In this study, effect of two variables one related to printing parameters and other depending on the sintering were selected. The printing parameter that was studied is the deposition strategy of successive layers. The stiffness and voids of parts printed by deposition modeling also depends upon the type layer deposition strategy adopted. A study showed different raster angles yield different results, and most commonly used strategy having raster angle of [45° / -45°] between successive layers still had voids as compared to raster angel [0° / 90°] as per study conducted by P. Kulkarni and D. Dutta (Kulkarni & Dutta, 1999)[10]. Raster angle is defined as the angle that the printing layers make with the horizontal axis of the print table. The deposition strategy studied in this research was the layer height. Layer

Height is the height of each layer deposited on the print table / successive layer. Different Layer Height yield different properties and is crucial for optimized result. Two deposition studies were studied one with each layer having 0.1 mm layer height while the other with 0.2 mm layer height. Cylindrical shape specimens with 25 mm diameter and 20 mm height were to be printed using the aforementioned layer deposition strategy.

The second variable corresponds to sintering time, three points / sintering durations were selected for study against each sample. The first during the initial phase that is 45 minutes after reaching the sintering temperature. Second and third one after 240 minutes (4 hours) and 360 minutes (6 hours) respectively of reaching the sintering temperature. A sintering temperature of 980 C^o was selected based on the instruction provided by Virtual Foundry and also found going through the literature available on sintering of copper. Similar thermal conditions were used by A. Vagnon et al. in study of copper sintering mechanism in situ by X-ray microtomography. Spherical copper particles having grain size 40 – 60 µm were placed in quartz capillary tube of 1 mm diameter and 20 mm length and sintered for 390 minutes (6.5 hours) at 1070 C^o (Vagnon, et al., 2008)[21]. Summary of conditions selected for study are listed in table.

Nomenclature	Diameter (mm)	Height (mm)	Sintering Temperature (C^o)	Layer Height (mm)	Sintering Time (min)
Specimen 1	25	20	980	0.2	45
Specimen 2	25	20	980	0.2	240
Specimen 3	25	20	980	0.2	360
Specimen 4	25	20	980	0.1	45
Specimen 5	25	20	980	0.1	240
Specimen 6	25	20	980	0.1	360

Table 3. 2: Design of Experiment Parameters

Chapter 4:   Sintering

4.1 Sintering Process

Sintering occurs when particles are heated to a temperature that is close to their melting point. The surface energy of particles is utilized in making bonds and adopting a structure that is more compact and denser. Sintering process can generally be classified in two types, 1) Solid State Sintering 2) Liquid Phase Sintering. As name depicts, Liquid phase sintering process is carried out on alloys and composite having a range of melting point hence solid particles coexist with a wetting liquid that helps in densification by pulling the solid grains together due to capillary force (German, Suri, & Park, 2009)[22]. No such liquid flow is present in solid state sintering. The current sintering process corresponds to solid-state sintering in which solid particles undergo fusion process. Figure 4.1 shows an illustration of the sintering process, at initial stage (a), the pore size comparatively greater and each grain has its definite boundary visible. At the intermediate stage (b), we can see particle fusing with each other and solid necks being created. The size of the pore has reduced significantly, such arrangement adds strength to the solid body. The last stage (c) is when the pore is eliminated by fusion of the particles as illustrated. In some cases, small voids may still remain in the solid body that is referred as the porosity.
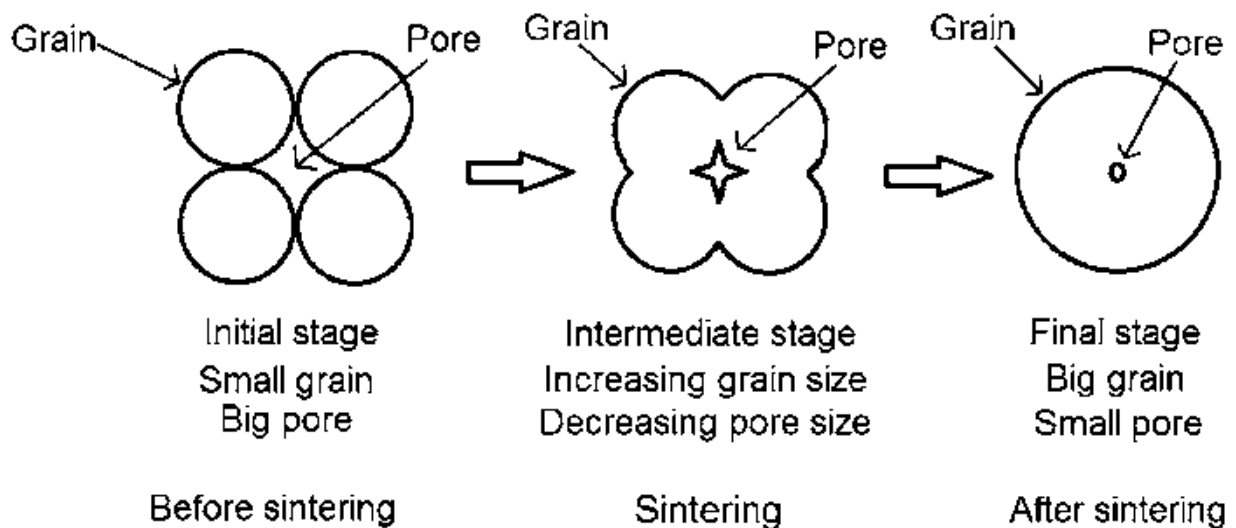
Figure 4. 1: Fused of Grains During Sintering Process

4.2 Sintering Furnace

The furnace used for sintering was a NABERTHERM open end furnace (Model N-17/HR) electrical furnace with a maximum temperature range of up to 1280 C^o that T_{max} shown in figure 4.2. The inner dimensions of the furnace were 250 mm width, 140 mm height and a depth of 500mm. For homogenous temperature in the whole furnace three side heating is done that is from both sides and bottom. The furnace allowed the input of firing of cycle and temperature consistency up to +/- 10 $C°$

Figure 4. 2: NABERTHERM Open End Furnace (Model N-17/HR)

4.3 Pre-Sintering Process for Non-Reactivity of Metal

To prevent oxidation / reaction of copper metal in the open environment, the green specimens were first suspended in a crucible full of sintering refractory ballast which was allowed to dry before the firing cycle. The crucible with submerged specimen is shown in figure 4.3, it was made sure at least a minimum of 10 mm thickness of the ballast was present around the specimen. This enabled the green part to preserve its shape even after sintering and also provided a localized inert / oxygen free environment in the furnace.
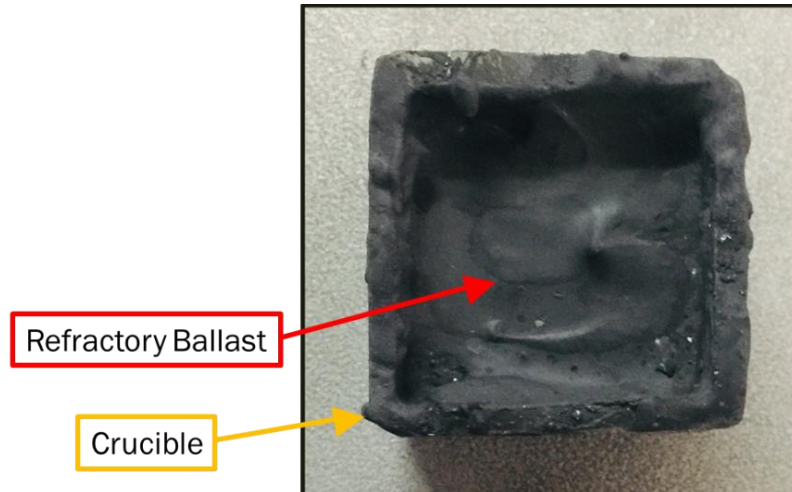
Figure 4. 3: Coupon Submerged in Refractory Ballast

4.4 Sintering Cycle

The sintering cycle for this study is given in figure 4.4. The candling and debinding parameters used in this study were those provided by OEM. The final sintering time however was changed as per defined in the DOE table 3.2. The general instructions for sintering cycle are as followed.

- Ramp the temperature to 150 C° as quickly as possible

- Hold the temperature at 150 C° for 75 minutes

- Ramp the temperature to 400 C° at a rate of 1.25 C° / minute

- Do not hold (if not possible hold for 1 minute)

- Ramp the temperature to 980 C° or selected sintering temperature at a rate of 3.25 C° / minute

- Hold the temperature for selected sintering time
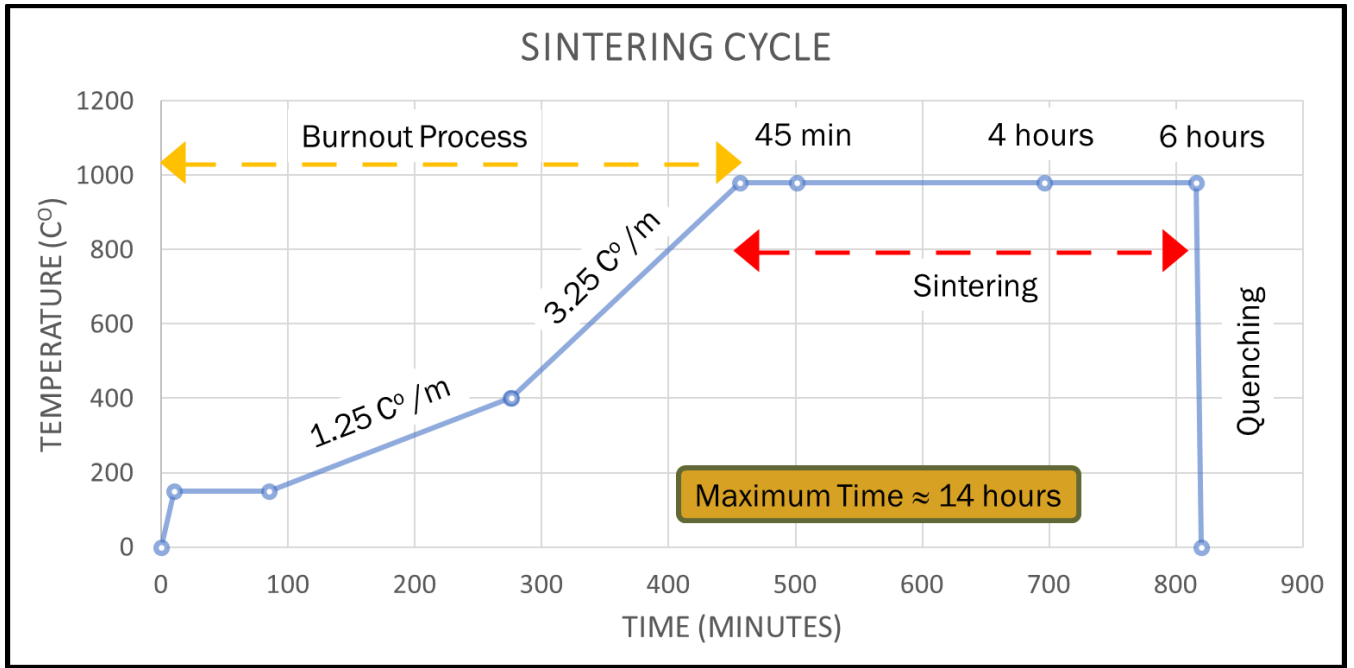
Figure 4. 4: Sintering Cycle

Chapter 5: Results and Discussions

Specimens after quenching were analyzed, layer of refractory ballast was still present after sintering. Presence of this layer verified that the process was inert and there was no reaction of metal with oxygen or other impurities. The shape of samples was also preserved and slight Brushing/polishing removed the outer layer. The sintered sample with external refractory ballast layer is shown in Figure 5.1. The black color is because of the refractory ballast layer.

Figure 5. 1: Sintered Sample with External Refractory Ballast Layer

5.1 Shrinkage

The dimensional shrinkage behavior of the specimen is shown in figure 5.2. Relatively larger shrinkage can be observed in 0.1 mm layer height specimens. This is because of more compact arrangement of copper grains in the green part. Secondly, relatively voids are present for 0.2 mm layer deposition strategy. The shrinkage in height is also more as compared to diameter shrinkage. The reason behind said is a small amount of weight/pressure on the specimen due to refractory blast above the specimen.
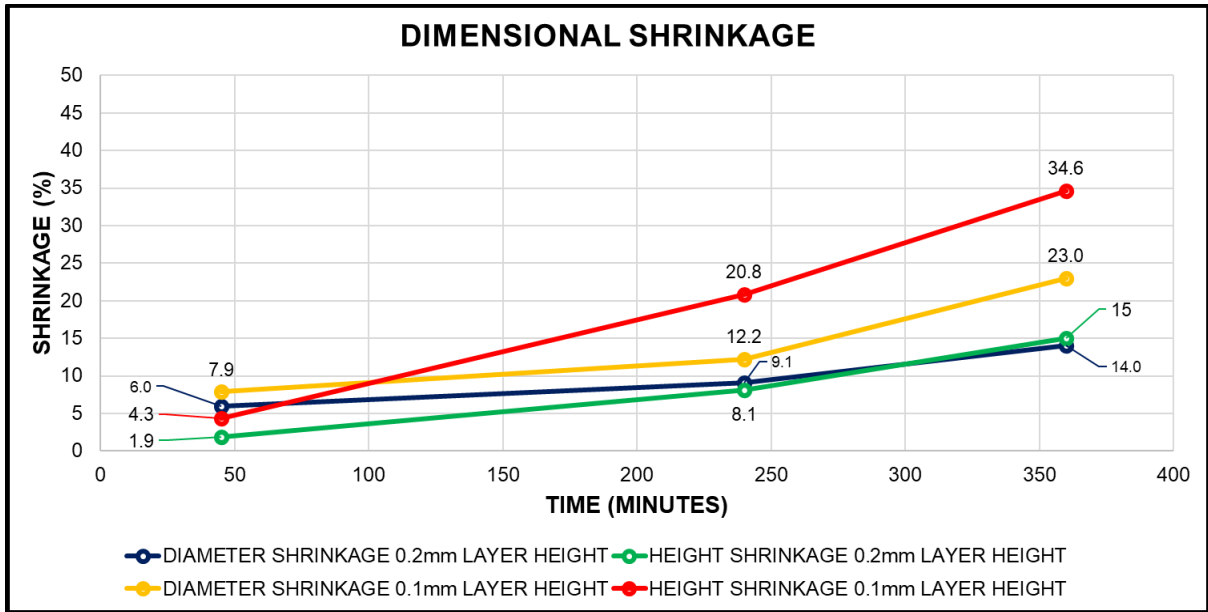
Figure 5. 2: Dimensional Shrinkage of Coupons

The overall volumetric shrinkage is shown in figure 5.3. The graph shows a maximum of 61.2 % & 37.1% shrinkage for 0.1 mm and 0.2 mm layer height coupons against 6 hours sintering time respectively.
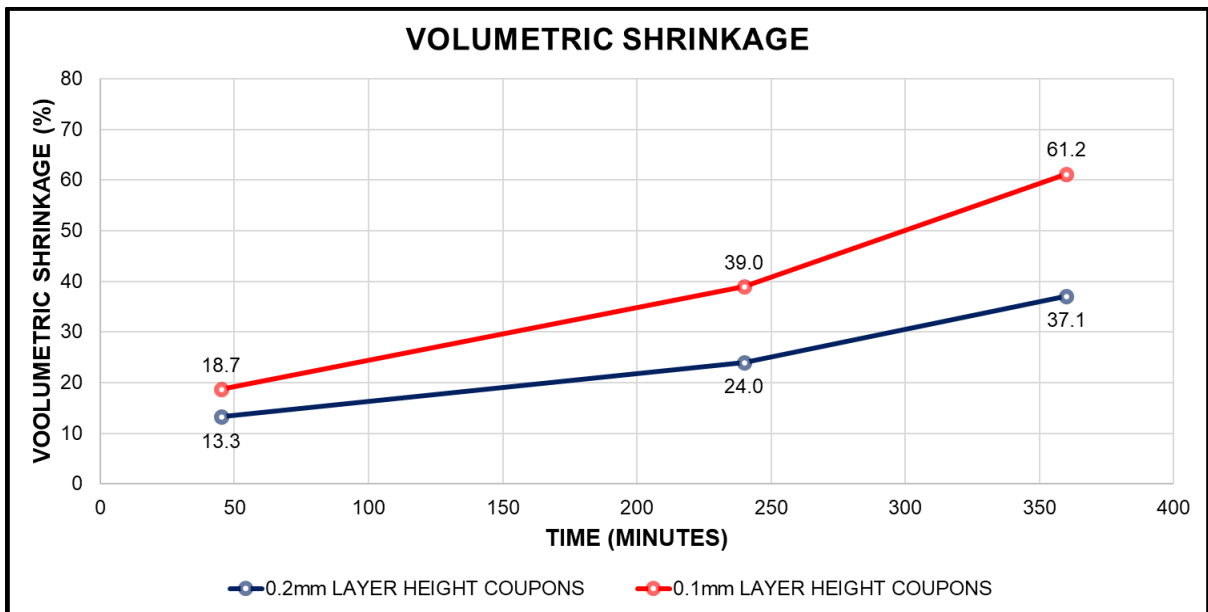
Figure 5. 3: Volumetric Shrinkage of Coupons

5.2 Metallography

Metallography was carried for the evaluation of obtained samples with regard to its structure. Samples were mounted using the hard-mounting technique in Bakelite. Subsequently, grinding and polishing was carried out for image analysis. The mounted sample is shown in figure 5.4.

Figure 5. 4: Copper coupon mounted in Bakelite

Following figures show the structure of different copper coupons at 100 µm obtained through digital microscope. Figures show how layer height can be the key parameter for parts prepared through fused deposition modelling technique.
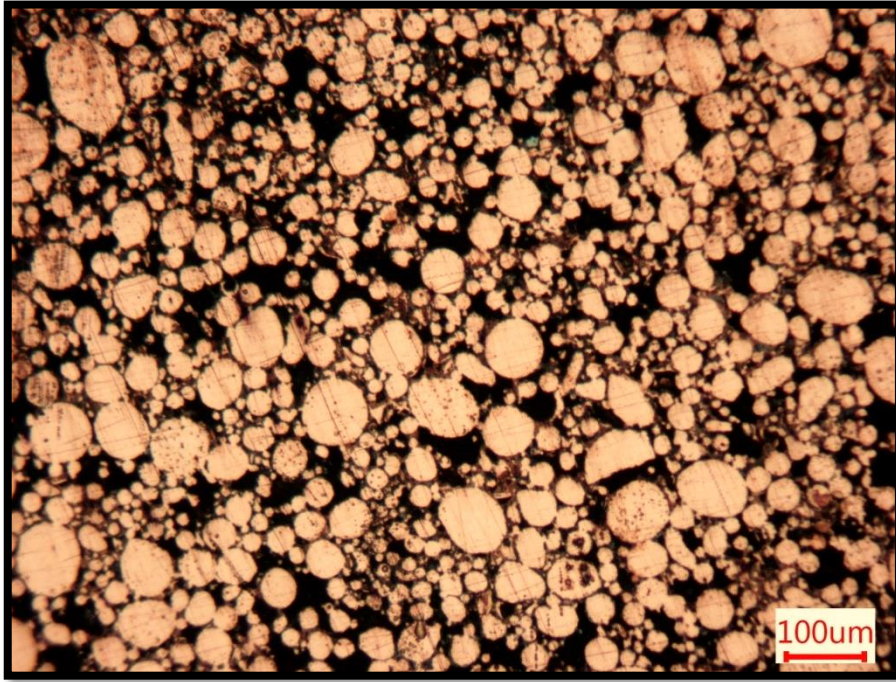
Figure 5. 5 0.2 mm Layer Height Copper Coupon after 45 minutes sintering

Figure 5. 6: 0.1 mm Layer Height Copper Coupon after 45 minutes sintering
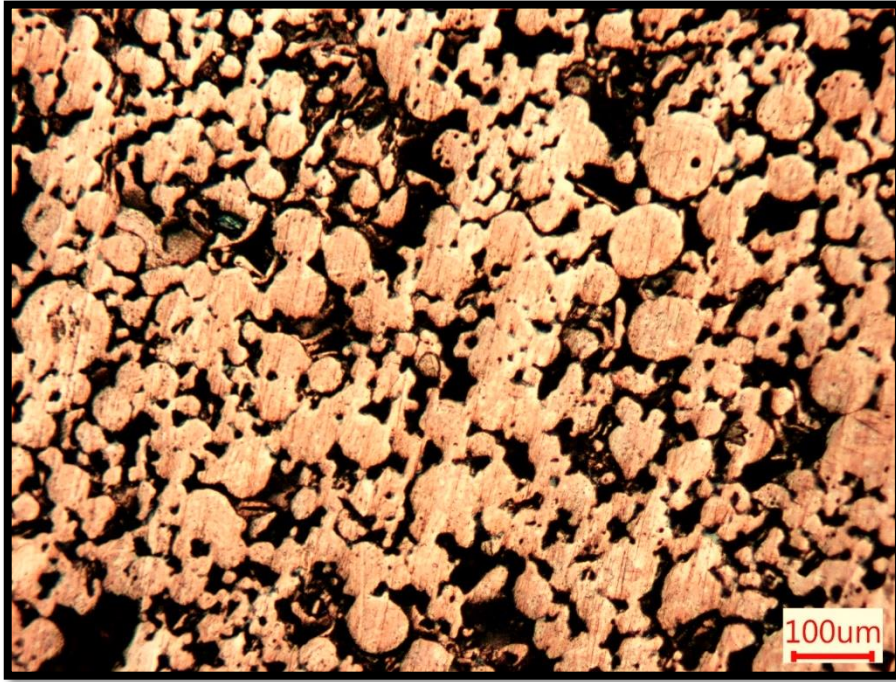
Figure 5. 7: 0.2 mm Layer Height Copper Coupon after 240 minutes sintering
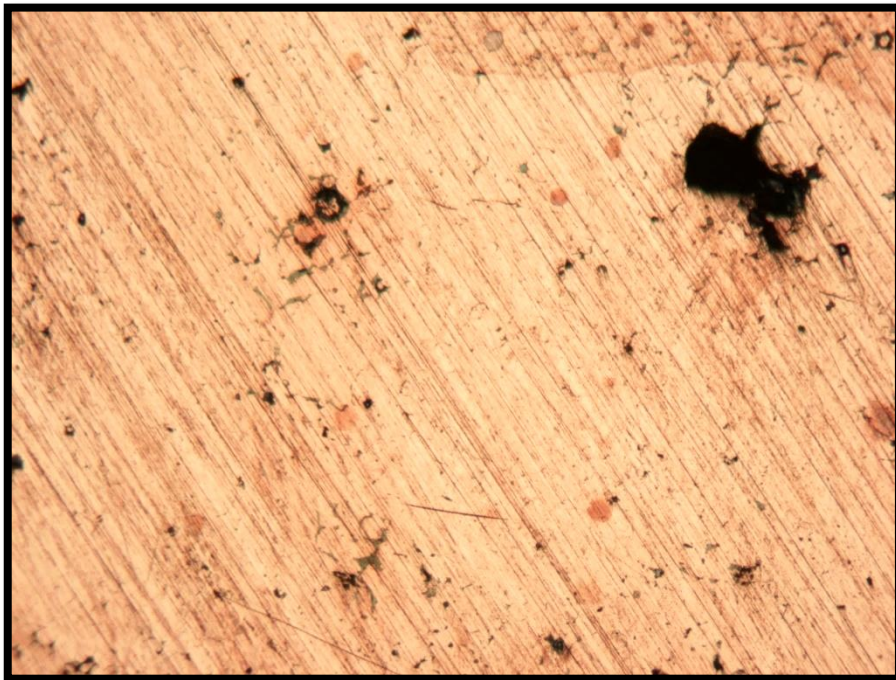
Figure 5. 8: 0.1 mm Layer Height Copper Coupon after 240 minutes sintering
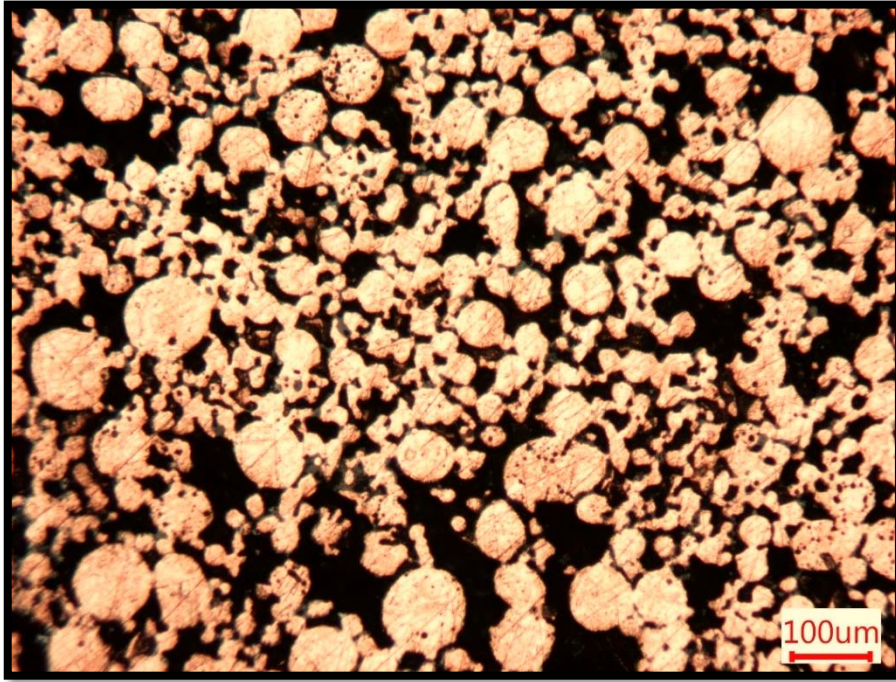
Figure 5. 9: 0.2 mm Layer Height Copper Coupon after 360 minutes sintering
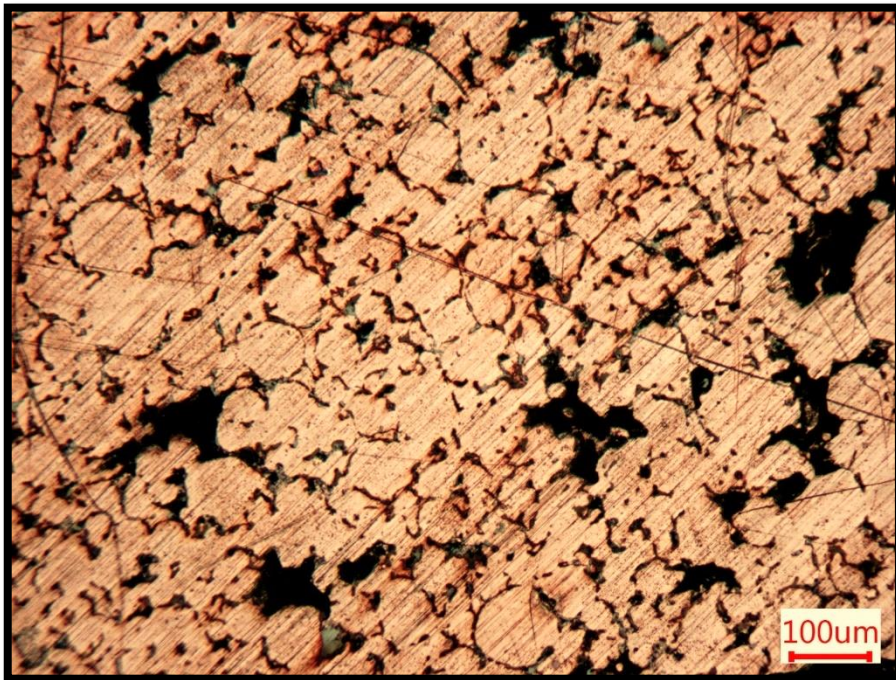
Figure 5. 10: 0.1 mm Layer Height Copper Coupon after 360 minutes sintering

5.3 Image Analysis

The algorithm used in this study for image analysis was obtained by modifying script developed by A. Rabbani et al. for extraction of pore network from 3-D Realistic Microtomography images (Rabbani, Jamshidi, & Salehi, 2014)[23]. The major functions used in the script are

> ➢ Morphological Transformation (Majority)
>
> ➢ Distance Mapping (City Block)
>
> ➢ Filtering for noise removal (Median)
>
> ➢ Segmentation (Watershed Algorithm)
>
> ➢ Region Detection (Regionprops)

The script can also be used on 2D images, simple image processing functions are used to characterize the image. The image is converted into a binary map of "0" and "1" where "1" highlight the presence of grain while "0" exhibits a pore or void. Initially opening and morphological function "Majority" was used for eliminating minor roughness and unwanted features. Afterwards, City-block distance function is used for distance mapping of the image. The equation which is used for calculating the distance via City-block is given as

$$D_b = |x_b - x_i| + |y_b - y_i|$$

Where (x_b, y_b) is the position of any random black pixel while (x_i, y_i) is the position of specific white pixel. In some cases, even after initial smoothening some noise may still be present, this noise may cause image processing algorithm to detect fake rigid lines. To avoid said issue median filtering is applied after the distance function. This technique is a nonlinear method and helps removing unwanted noise from the image. The pixel value is replaced with a median value in the (m x n) neighborhood. One advantage of median filtering technique over other similar techniques is it saves distinct edges rather than making unrealistic pixels. used to remove noise from images. Subsequent to median filtering, watershed segmentation algorithm is applied to detect and separate the grains and pores from the image. The algorithm treats the image as a surface with pixel having value "1" represent high elevation while the pixels having value "0" represent low elevation. A number of watershed regions are made each representing a unique region except elements labeled 0.

The watershed algorithm uses 8-connected neighborhoods for 2-D images while 3-D inputs has a default value of 26-connected neighborhoods. Watershed was applied for microstructure evaluation whereas script was modified to compute copper accumulation using the region detection function. An example of the region detection script is shown in figure x.
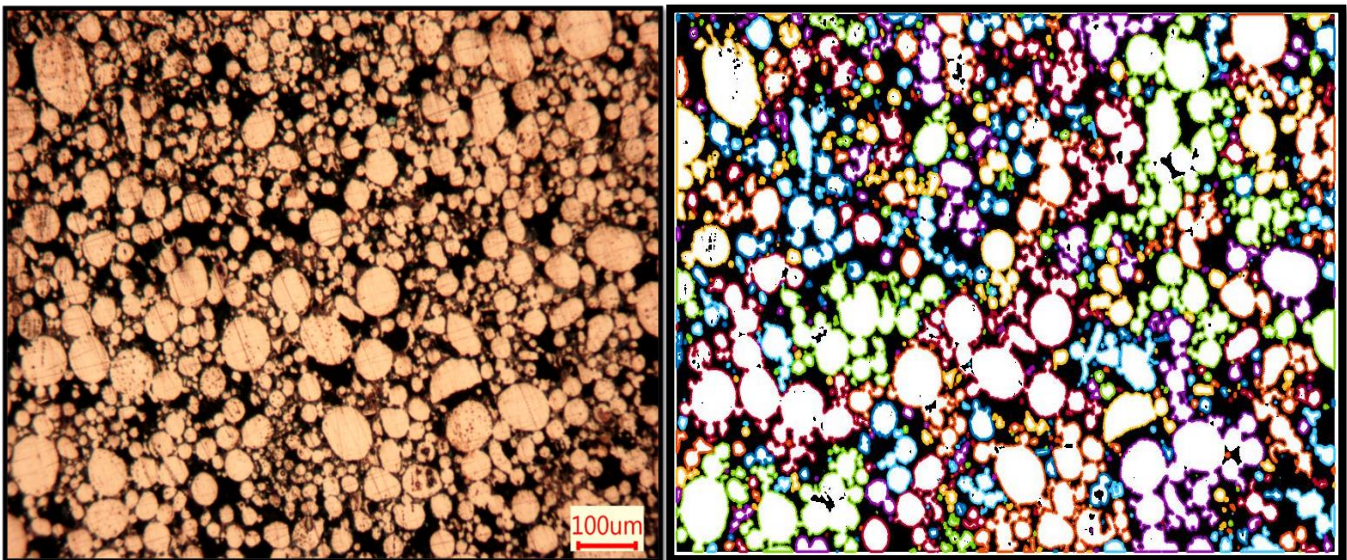

Figure 5. 11: *Detected Copper Accumulation Regions using MATLAB Script*

5.3.1 Copper Accumulation Distribution

Following figure show the distribution of copper accumulation in different samples using the region prop function. The function considers the area a single region if it is connected via a small link.
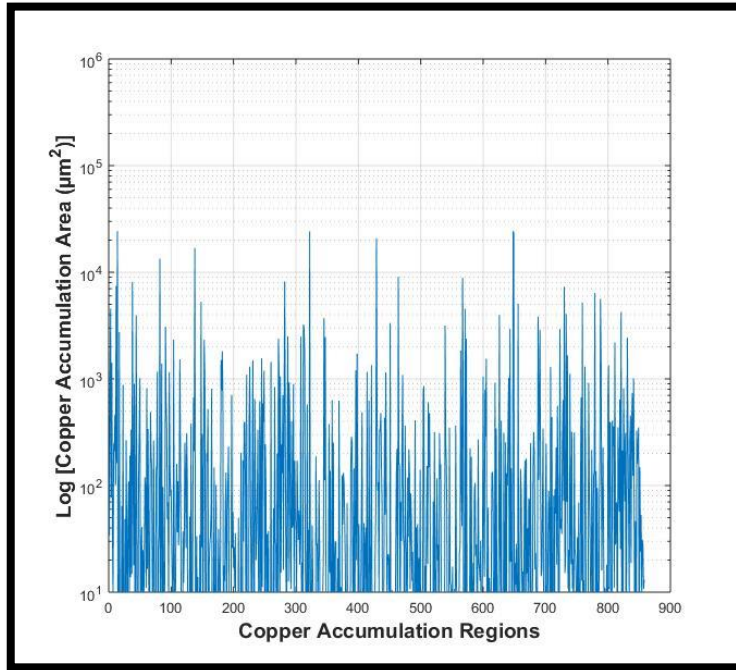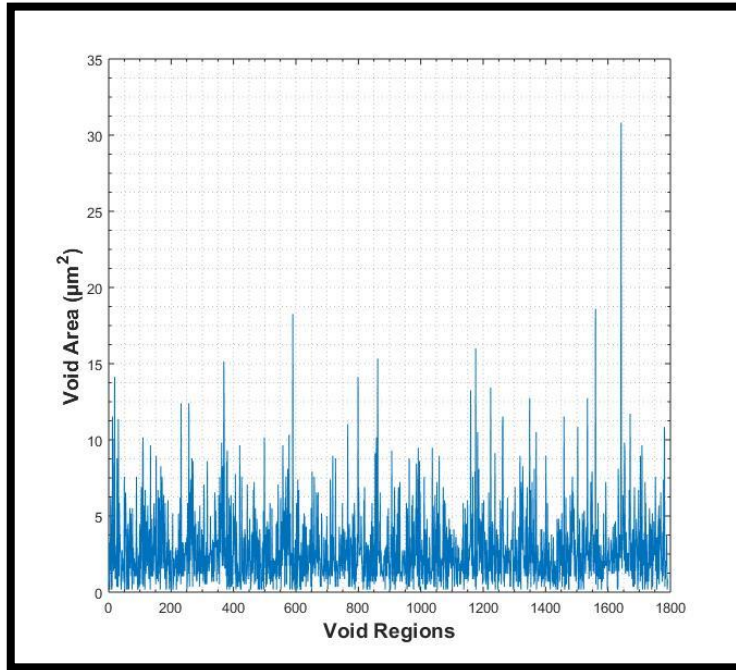
Figure 5. 12: Copper Distribution in 0.2 mm Layer Height & 45 Minutes Sintered Coupon
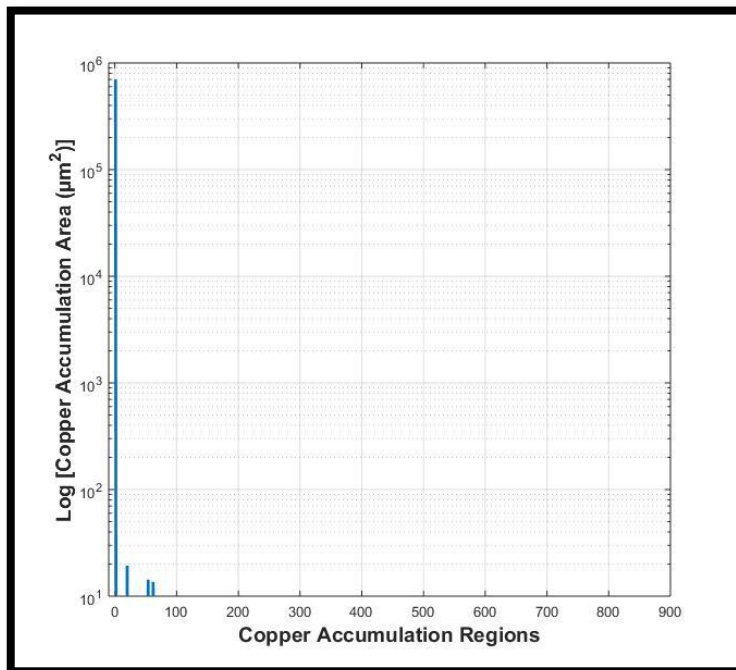
Figure 5. 13: Copper Distribution in 0.1 mm Layer Height & 45 Minutes Sintered Coupon
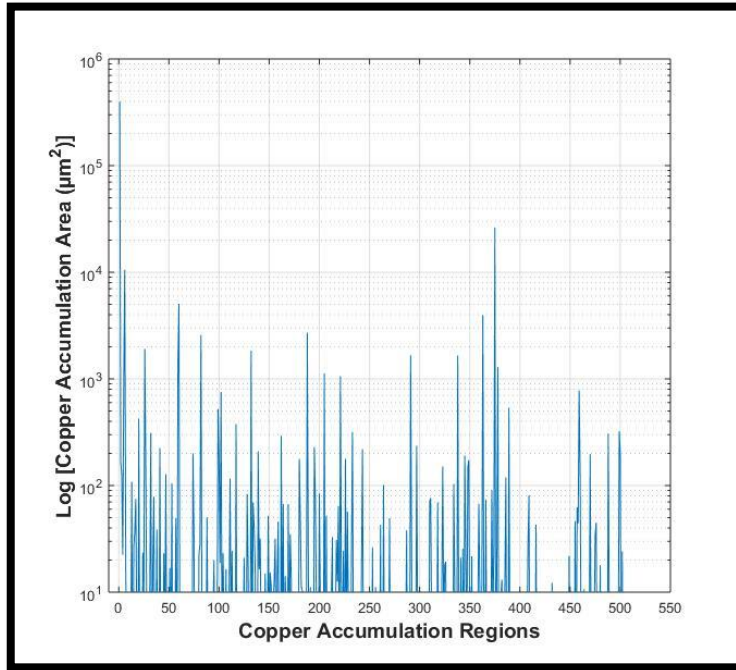
Figure 5. 14: Copper Distribution in 0.2 mm Layer Height & 240 Minutes Sintered Coupon
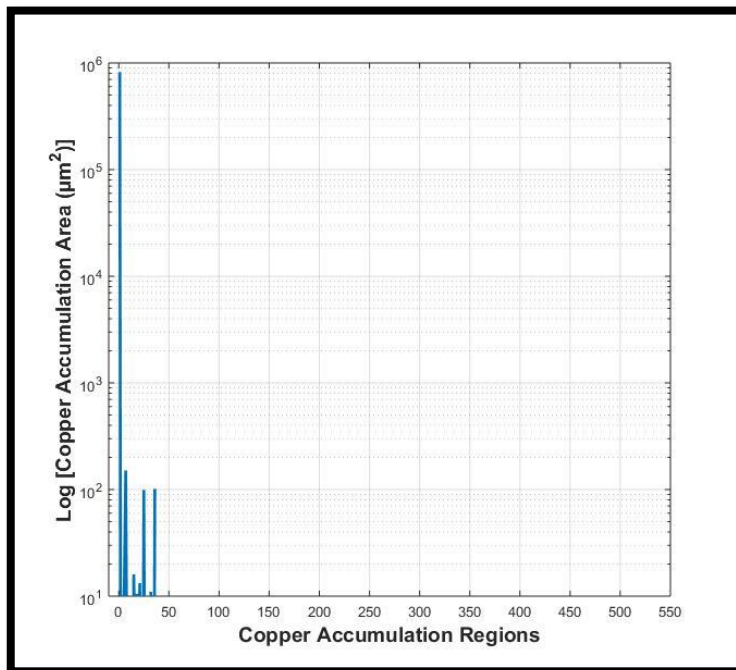
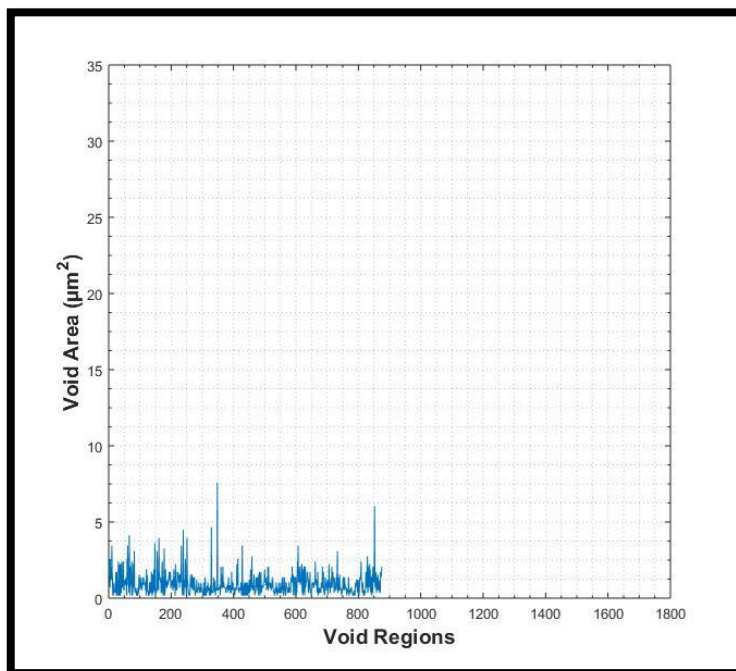**Figure 5. 15:** Copper Distribution in 0.1 mm Layer Height & 240 Minutes Sintered Coupon
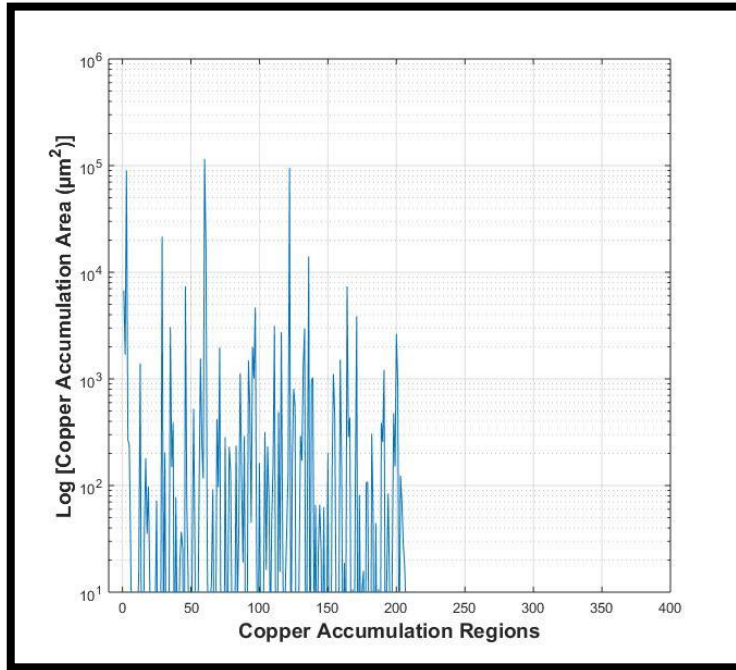
Figure 5. 16: Copper Distribution in 0.2 mm Layer Height & 360 Minutes Sintered Coupon
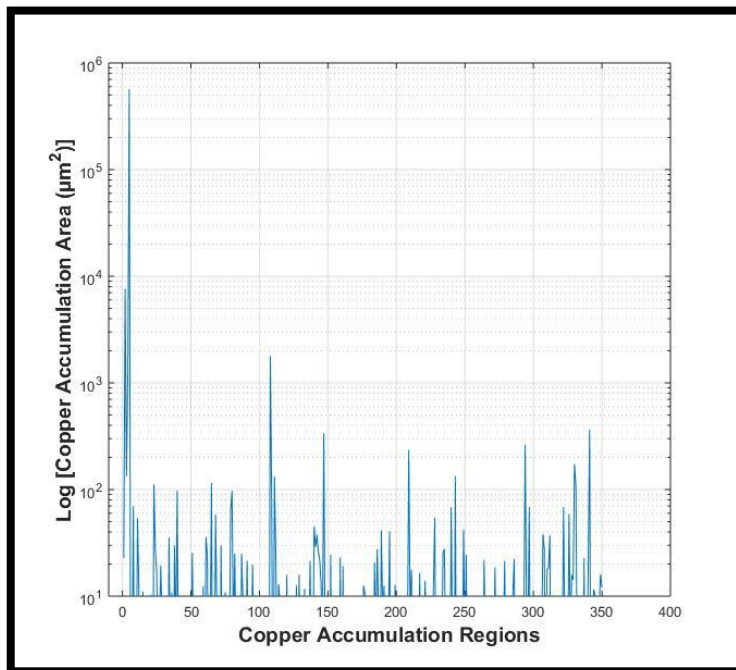
Figure 5. 17: Copper Distribution in 0.1 mm Layer Height & 360 Minutes Sintered Coupon

The maximum copper accumulated area in different samples is shown in figure 5.18. we can see that the connected area in case of 0.1 mm layer height is greater than 90 %.
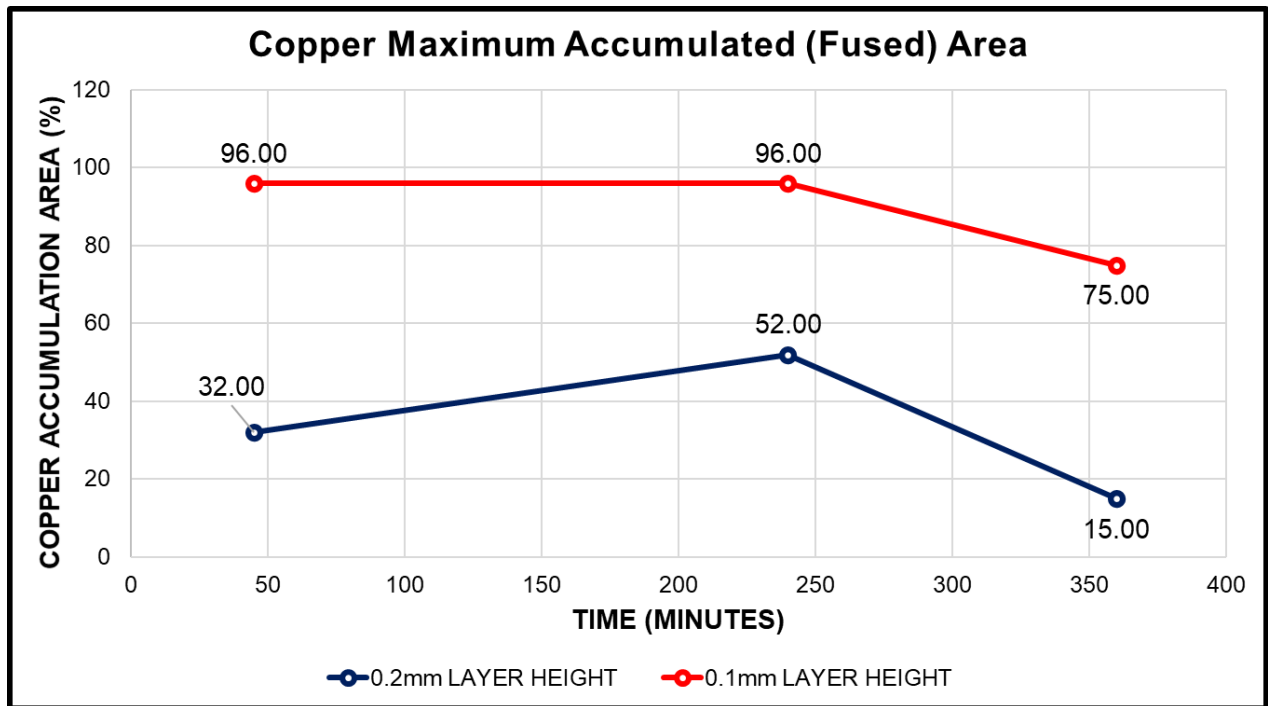
Figure 5. 18: Maximum Copper Accumulation Area

5.3.2 Throat Size Distribution

Using this script pore size distribution at each time duration was also obtained. Rather than using region prop watershed was used for this purpose. Following figures show the throat size distribution for the obtained samples.

Figure 5. 19: Throat Area Distribution in 0.2 mm Layer Height & 45 Minutes Sintered Coupon

Figure 5. 20: Throat Area Distribution in 0.1 mm Layer Height & 45 Minutes Sintered Coupon
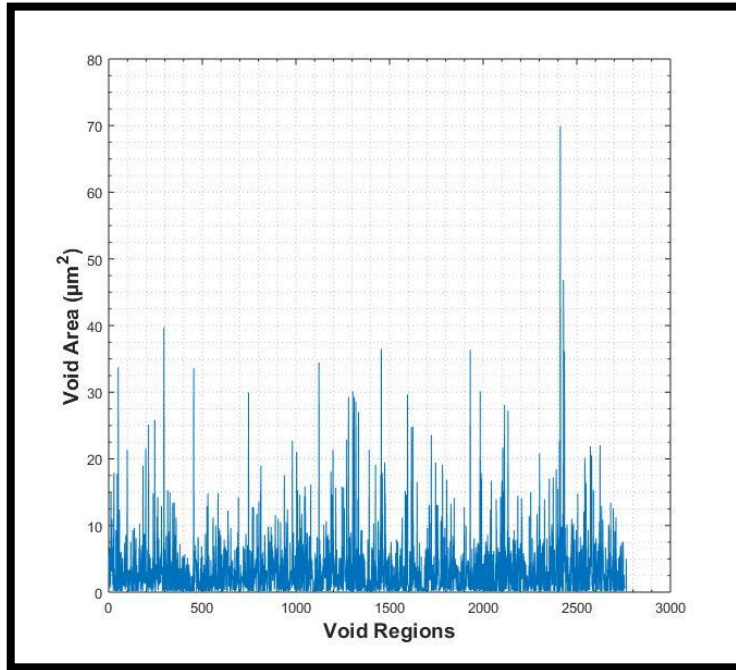
Figure 5. 21: Throat Area Distribution in 0.2 mm Layer Height & 240 Minutes Sintered Coupon
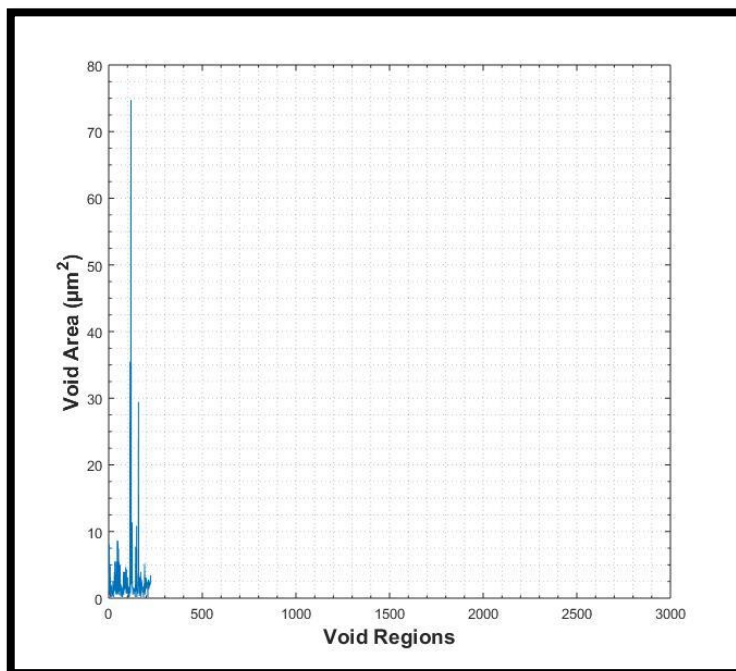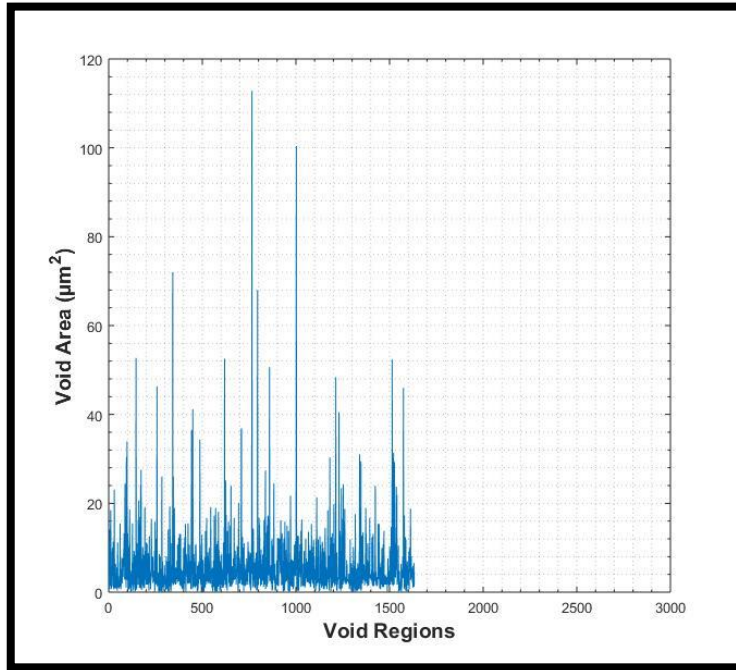

Figure 5. 22: Throat Area Distribution in 0.1 mm Layer Height & 240 Minutes Sintered Coupon

Figure 5. 23: Throat Area Distribution in 0.2 mm Layer Height & 360 Minutes Sintered Coupon
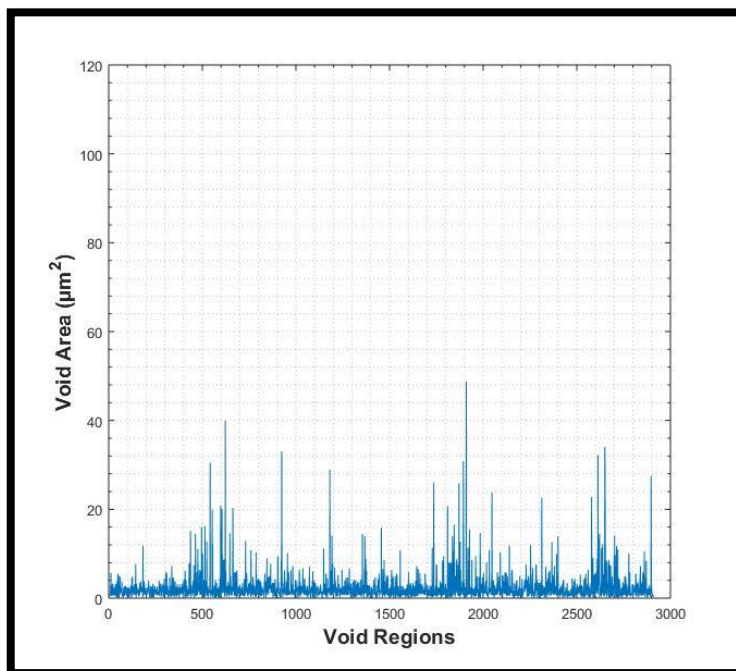

Figure 5. 24: Throat Area Distribution in 0.2 mm Layer Height & 45 Minutes Sintered Coupon

The mean void area for the tested coupons is shown in figure 5.25. A sharp rise in the void area can be observed after 4 hours sintering time for both 0.1 mm and 0.2 mm layer height coupons.
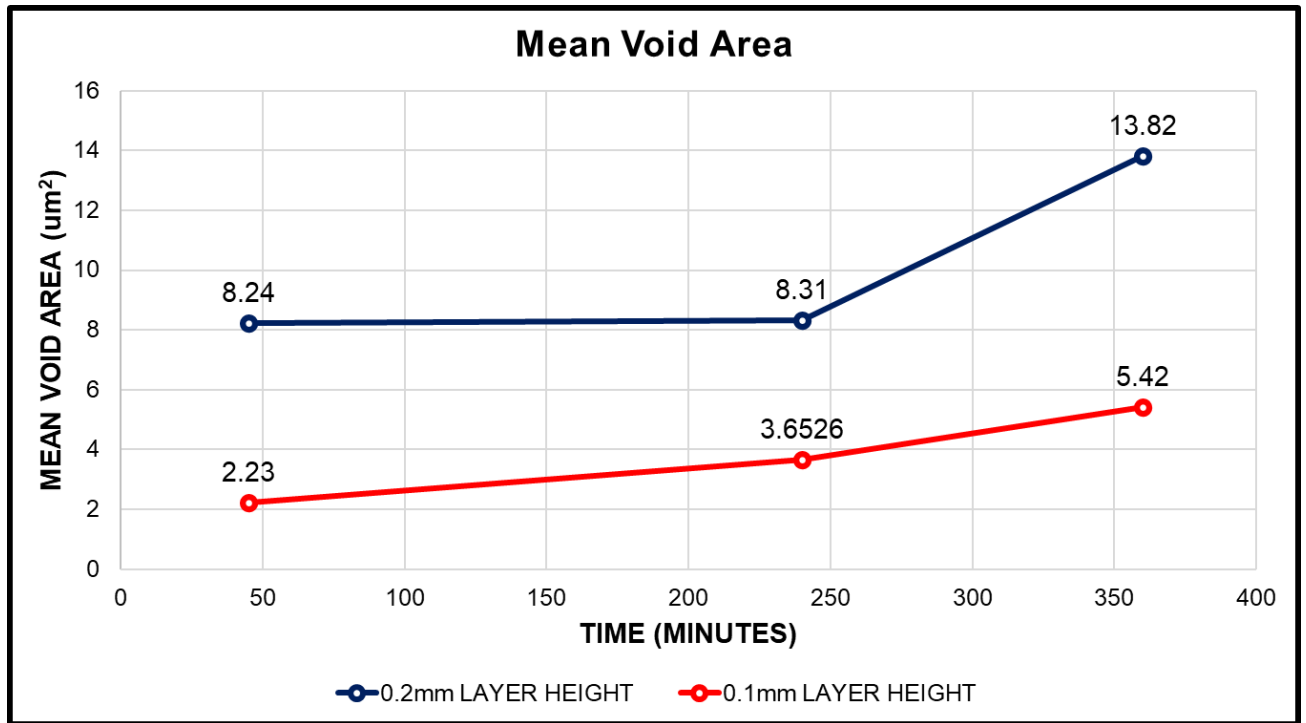

Figure 5. 25: Mean Void Area for Copper Coupons

5.3.3 Density Calculation

Image analysis was also used for determining the density of the specimens. The image analysis technique determines the density based on the area percentage of pores present on the specimen surface prepared by metallography.
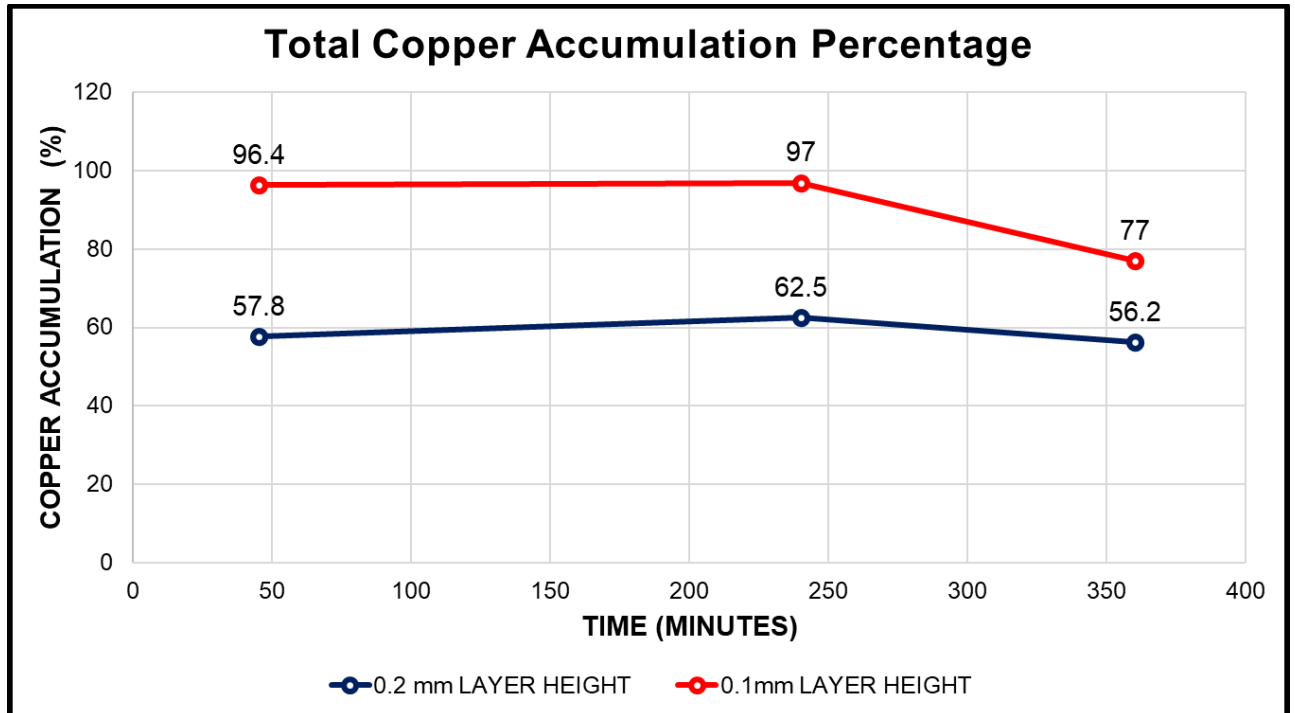
Figure 5. 26: Density of Copper Coupons

5.4 Micro Hardness

Micro vicker hardness test were carried out to evaluate hardness of obtained samples. The Vickers test is often easier to use than other hardness tests since the required calculations are
independent of the size of the indenter, and the indenter can be used for all materials irrespective
of hardness. Micro hardness of 0.2 mm layer height coupons was not possible due to large void areas. Five value of vicker hardness for each 0.1 mm layer height coupon were taken. The procedure adopted was as followed.

➢ Placed the prepared specimen on the micro Vickers hardness tester bed

➢ Switch-on the tester and rotate the lens turret to position on the specimen

➢ Turn indenter turret on the specimen and then apply the force When the start button is press, the tester will first load, then dwell, and finally unload

➢ Measure the diamond shape indentation display in the machine lens

➢ Input the average length of the diagonal of the diamond shape to the tester

> Repeat to test at different regions of the specimen then shut down the tester and remove the specimen

Figure 5.27 shows the indentation of 0.1 mm layer height and 4 hours sintered sample. The load used for the test was 100g and dwell time was set to 15 seconds.
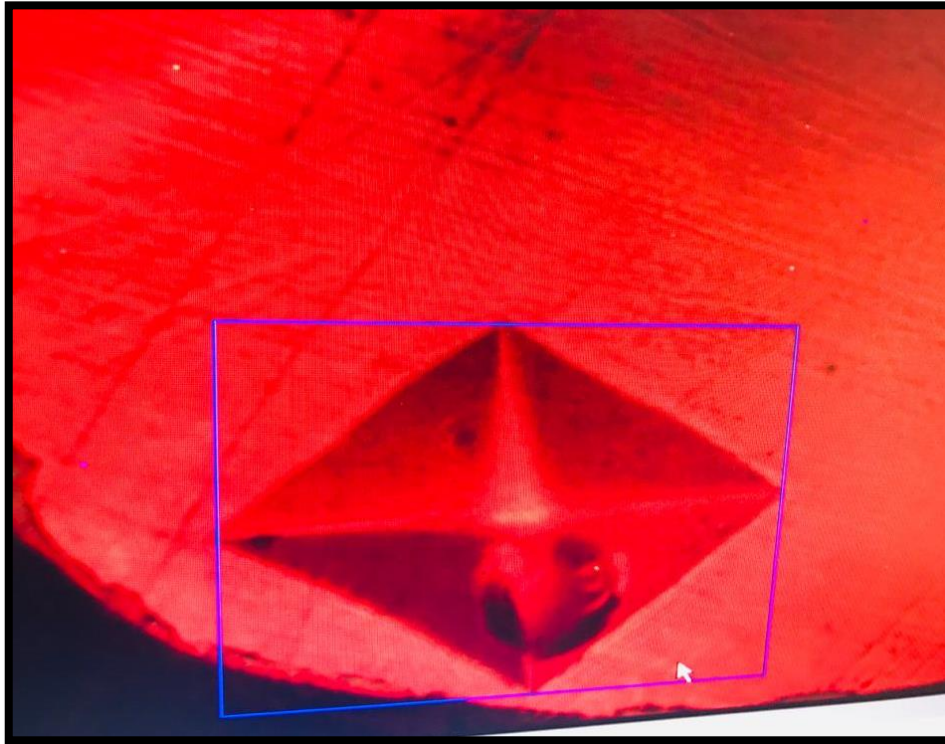

Figure 5. 27: Micro Vicker Testing – Indent for max 85.8 HV value

Figure 5.28 shows average hardness values for different copper coupons. The maximum value is obtained for the 0.1 mm layer height and 4 hours sintered sample.
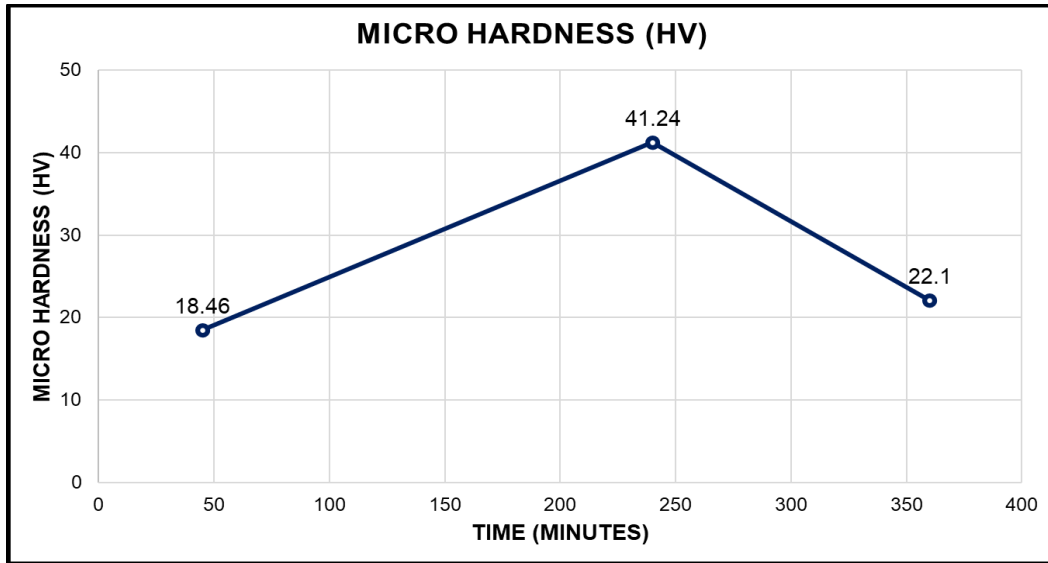
Figure 5. 28: Average Microhardness values for 0.1 mm Layer Height Coupons

5.5 Optical Emission Spectroscopy

Optical Emission Spectroscopy, or OES analysis, is a rapid method for determining the elemental composition of a variety of metals and alloys. OES analysis uses a sparking process, which involves applying an electrical charge to the sample, vaporizing a small amount of material. Once this spark occurs, a discharge plasma with a distinct chemical signature is created, allowing evaluation of exact, quantitative breakdown and elemental breakdown of solid material. Results of the analysis are given as a percentage breakdown of the constituent elements. Table 5.1 shows the breakdown composition of coupons obtained through OES.

Element	0.2 mm Layer Height			0.1 mm Layer Height		
Time	45	240	360	45	240	360
Cu	97.83	99.70	99.95	97.26	99.61	99.83
Sn	.0057	.0048	.0036	.0052	.0041	.0032
Pb	.013	.003	<.001	.016	.002	<.001
Zn	.046	.015	<.001	.050	<.001	<.001
Ni	.017	<.001	<.001	.023	.014	.01
Mn	<.001	.0018	<.0003	.0090	<.001	<.001

Table 5. 1: Composition of Coupons after sintering

Chapter 6: Conclusions and Future Works

This chapter includes a conclusive argument established on the results inferred from the previous chapters which explains the essence of the research work carried out and the objective requirements that were to be fulfilled.

The study was carried out to optimize the process of preparing metal parts through fused deposition modelling technique, a number of experiments were carried which yielded the following conclusions.

- Coupon 5 with 0.1 mm layer height and 4 hours sintering time yielded the optimum results

- Microstructure and micro-hardness value 41.24 HV at aforementioned condition (coupon 5) was comparable with that of casted copper that is 50 HV for annealed copper while 100 HV for cold worked copper

- Minimum porosity value of 3.14 % was observed based on the image analysis for optimum condition making it an adoptable technique

- Layer Height has immense effect on the microstructure of the final results, larger value tends to greater voids/gaps

- Maximum Sintering duration at 980 C^o should not be greater than 4 hours. Sintering of coupons for durations more than 4 hours causes disintegration

- Composition test shows > 99.5 % of copper in end product which validates the burnout process adopted for PLA removal

- Volumetric Shrinkage was greater than defined by OEM and needs to be catered during the CAD model through hit and trial procedure

- Non-Homogenous shrinkage with respect height and diameter was observed

- Future study should include studying the effect of physical dimension on output

References

1. Additive, G. (2020). *How Direct Metal Laser Melting (DMLM) Works*. Retrieved from Direct Metal Laser Melting (DMLM) | GE Additive: https://www.ge.com/additive/additive-manufacturing/information/direct-metal-laser-melting-technology

2. Agarwala, M., Weeren, R. v., Bandyopadhyay, A., Whalen, P., & Safari, A. S. (1996). Fused Deposition of Ceramics and Metals : An Overview. *1996 International Solid Freeform Fabrication Symposium.*

3. Arivarasi, A., & Kumar, A. (2016). 3D Printing of Copper Filament for Layered Fabrication. *WSEAS Transactions on Electronics, 7.*

4. *Electron Beam Melting.* (2020). Retrieved from Additively: https://www.additively.com/en/learn-about/electron-beam-melting#read-advantages

5. Frazier, W. (2014). Metal Additive Manufacturing: A Review. *Journal of Materials Engineering and Performance, 23*, 1917-1928.

6. German, R., Suri, P., & Park, S. (2009). Review: liquid phase sintering. *Journal of Materials Science, 44*, 1-39.

7. Giberti, H., Strano, M., & Annoni, M. (2016). An innovative machine for Fused Deposition Modeling of metals and advanced ceramics. *2016 4th International Conference on Nano and Materials Science (ICNMS 2016). 43.* MATEC Web of Conferences. doi:10.1051/matecconf/20164303003

8. Gokuldoss, P. K., Kolla, S., & Eckert, J. (2017). Additive Manufacturing Processes: Selective Laser Melting, Electron Beam Melting and Binder Jetting-Selection Guidelines. *Materials*, 672.

9. Guohua, W., Noshir A., L., Rajendra, S., & Danforth, S. (2002). Solid freeform fabrication of metal components using fused deposition of metals. *Materials & Design, 23*(1), 97-105. doi:https://doi.org/10.1016/S0261-3069(01)00079-6.

10. Jung, H. Y., Choi, S. J., Prashanth, K. G., Stoica, M., Scudino, S., Yi, S., . . . Eckert, J. (2015). Fabrication of Fe-based bulk metallic glass by selective laser melting: A parameter study. *Materials & Design, 86*, 703-708. doi:10.1016/j.matdes.2015.07.145

11. Kimura, T., Nakamoto, T., Mizuno, M., & Araki, H. (2017). Effect of silicon content on densification, mechanical and thermal properties of Al-xSi binary alloys fabricated using selective laser melting. *Materials Science and Engineering: A*, 593-602. doi:10.1016/j.msea.2016.11.059

12. Kulkarni, P., & Dutta, D. (1999). Deposition Strategies and Resulting Part Stiffnesses in Fused Deposition Modeling. *ASME. J. Manuf. Sci. Eng., 121*(1), 93-103. doi:10.1115/1.2830582

13. Laakso, P., Riipinen, T., Laukkanen, A., Andersson, T., Jokinen, A., Revuelta, A., & Ruusuvuori, K. (2016). Optimization and Simulation of SLM Process for High Density H13 Tool Steel Parts. *Physics Procedia, 83*, 26-35. doi:10.1016/j.phpro.2016.08.004

14. Langrana, W. G., Rangarajan S, N., & al., e. (1999). Fabrication of metal components using FDMet: Fused Deposition of Metals. *Proceedings of the Solid Freeform Fabrication Symposium* (pp. 775-782). Austin, TX: The University of Texas at Austin.

15. Liu, B., Wang, Y., Lin, Z., & Zhang, T. (2020). Creating metal parts by Fused Deposition Modeling and Sintering. *Materials Letters, 263*. doi:10.1016/j.matlet.2019.127252

16. Lu, Y., Wu, S., Gan, Y., Huang, T., Yang, C., Junjie, L., & Lin, J. (2015). Structure on the microstructure, mechanical property and residual stress of SLM Inconel-718 alloy manufactured by differing island scanning strategy. *Optics & Laser Technology, 75*, 197-206. doi:10.1016/j.optlastec.2015.07.009

17. Masood, S., & Song, W. (2004). Development of new metal/polymer materials for rapid tooling using Fused deposition modelling. *Materials & Design, 25*(7), 587-594. doi:10.1016/j.matdes.2004.02.009

18. McNulty, T., Cornejo, I., Mohammadi, F., Danforth, S. C., & Safari, A. (1998). Development of a Binder Formulation for Fused Deposition od Ceramics. *Proceedings of the Solid Freeforrn Fabrication Symposium*, (pp. 613-620).

19. Meiners, W. (2011). Fabrication Selective Laser Melting -Additive Manufacturing for series production of the future. *Proceedings of INTERMAT Conference.*

20. Mireles, J., Kim, H., Hwan Lee, I., Espalin, D., Medina, F., MacDonald, E., & Wicker, R. (2013). Development of a Fused Deposition Modeling System for Low

Melting Temperature Metal Alloys. *ASME.J. Electron. Packag., 135*(1). doi:10.1115/1.4007160

21. Nikzad, M., Masood, S. S., & Groth, A. (2007). Thermo-Mechanical Properties of a Metal-filled Polymer Composite for Fused. *5th Australasian Congress on Applied Mechanics, ACAM 2007.* Brisbane, Australia.

22. Prashanth K.G., S. S. (2015). Production of high strength Al85Nd8Ni5Co2 alloy by selective laser melting. *Additive Manufacturing, 6*, 1-5. doi:doi: 10.1016/j.addma.2015.01.001

23. Rabbani, A., Jamshidi, S., & Salehi, S. (2014). An automated simple algorithm for realistic pore network extraction from micro-tomography images. *Journal of Petroleum Science and Engineering, 123*, 164-171. doi:10.1016/j.petrol.2014.08.020

24. Riecker, S., Clouse, J., Studnitzky, T., Andersen, O., & Kieback, B. (2016). Fused deposition modeling-opportunities for cheap metal AM. *Powder Metallurgy World Congress & Exhibition.* Shrewsbury.

25. Schwab, H., Prashanth, K., Löber, L., Kühn, U., & Eckert, J. (2015). Selective Laser Melting of Ti-45Nb Alloy. *Metals, 5*, 686-694.

26. Thijs, L., Verharghe, F., Craeghs, T., Humbeeck, J., & Kruth, J.-P. (2010). A study of the microstructural evolution during selective laser melting of Ti-6Al-4V. *Acta Materialia*, 3303-3312. doi:10.1016/j.actamat.2010.02.004

27. University, L. (n.d.). *About Additive Manufacturing.* Retrieved from Binder Jetting | Additive Manufacturing Research Group | Loughborough University: http://www.lboro.ac.uk/research/amrg/about/the7categoriesofadditivemanufacturing/binderjetting/

28. Vagnon, A., Rivière, J., Missiaen, J., Bellet, D., Michiel, M. D., Josserond, C., & Bouvard, D. (2008). 3D statistical analysis of a copper powder sintering observed in situ by synchrotron microtomography. *Acta Materialia, 56*(5), 1084-1093. doi:10.1016/j.actamat.2007.11.008

29. Zhu, Y., Chen, X., & Yang, H. (2016). Tribology of selective laser melting processed parts: Stainless steel 316L under lubricated conditions. *Wear*, 46–55. doi:10.1016/j.wear.2016.01.004

Plagiarism Report